

# Is Trend Still Your Friend?

A Microstructural Account of the Demise of Short-Term Trend-Following

Jutta G. Kurth<sup>1, 2</sup>, Zoltan Eisler<sup>3</sup>, Adam Rej<sup>4</sup>, and Jean-Philippe Bouchaud<sup>4, 1, 5</sup>

<sup>1</sup>Econophysics Lab, Institut Louis Bachelier, 28 Place de la Bourse, 75002 Paris, France

<sup>2</sup>LadHyX UMR CNRS 7646, École polytechnique, 91128 Palaiseau Cedex, France

<sup>3</sup>Imperial College London, Department of Mathematics

<sup>4</sup>Capital Fund Management, 23 Rue de l'Université, 75007 Paris, France

<sup>5</sup>Académie des Sciences, 23 Quai de Conti, 75006 Paris, France

July 3, 2026

## Abstract

Systematic trend following has, on average, been profitable for at least two centuries; yet since approximately 2009, short-term trends have ceased to deliver reliable returns. Using a cross-section of roughly 100 liquid futures contracts spanning 1995–2025, together with an industry-representative CTA proxy, we document the break and characterise its dependence on signal speed and asset class. We evaluate four candidate explanations – capacity constraints, market electronication, a regime change in CTA-versus-order-flow interactions, and a microstructural mechanism – and find that the first three fail on grounds of timing, magnitude, or cross-sectional heterogeneity.

Our central empirical finding is that the cross-sectional variable distinguishing degraded from surviving trends is the *volatility-normalised tick size*: post-2008 trend PnL has collapsed on small-tick contracts across all signal horizons, while remaining essentially intact on large-tick contracts. Neither asset class nor liquidity replicates this dichotomy.

We interpret this result through the lens of a self-fulfilling feedback loop that, in our view, lies at the heart of the trend anomaly itself: *Trend signals trigger directional trades, whose market impact reinforces the very price moves that generated the signal*. The profitability and the persistence of trend are therefore both sustained by the same impact channel. This loop, however, requires that trend followers can actually execute aggressively at reasonable cost. We argue that the post-crisis transition to HFT-dominated market making, whose liquidity-withdrawal behaviour in the face of predictable directional flow has sharply contrasting consequences for sparse (small-tick) and dense (large-tick) limit order books, has broken this loop on small-tick contracts. On large-tick contracts, where residual depth remains sufficient, the loop continues to operate and trend continues to deliver. A complementary price-impact analysis shows that passive execution offers no escape, since it forfeits the self-reinforcement channel while incurring adverse opportunity costs.

**Keywords:** Trend following, CTA, market microstructure, tick size, high-frequency trading, market making, price impact.

## 1 Introduction

Few empirical regularities in finance have proven as persistent and as puzzling as the tendency of asset prices to trend. The observation that recent winners outperform recent losers contradicts the most basic tenet of the Efficient Market Hypothesis of Fama (1970) – obvious information (past trends) is not incorporated into prices. Yet the statistical evidence is overwhelming, spanning virtually every liquid market and stretching back at least two centuries, as shown by Lempérière et al. (2014); Hurst et al. (2017). Moskowitz et al. (2012) document “time-series

momentum” across 58 instruments and three and a half decades; market-neutral momentum in the stock space is also well known (Jegadeesh and Titman, 1993); further work by Baltas and Kosowski (2013), Levine and Pedersen (2016), and others has solidified trend following as one of the most robust anomalies ever documented in finance.

The commercial exploitation of this anomaly through the Commodity Trading Advisor (CTA) industry took off in the 1970s and 1980s, and by the 1990s had converged on a fairly homogeneous methodology: take positions proportional to the difference between a fast and a slow moving average of prices, normalised by volatility, diversified across as many liquid futures contracts as possible.

And yet, since approximately 2008/9, this anomaly appears to have been struggling, at least when looking at the performance of the SG CTA Index (the industry-standard benchmark for large CTAs) from 2000 to 2025; see Fig. 1. The contrast between the pre- and post-2008/9 regimes is stark: after nearly a decade of steady gains, performance has been effectively flat or negative for the past fifteen years, only saved by two macro-driven punctuations in 2014 and during Covid. A clean methodological proxy that we construct below paints the same picture with both sharper resolution and more nuance.



Figure 1: (Rebased) SG CTA Index, 2000–2025. Data courtesy of Société Générale Prime Services & Clearing.

Several stylised facts can be established and constrain any candidate explanation: (i) the break is *abrupt*, with the character of a structural regime shift rather than gradual alpha decay; (ii) it is *speed-dependent*, with fast signals (horizons of days to weeks) most affected whereas slow ones are approximately intact; (iii) it is *asset-class heterogeneous*, sparing yields and most commodities (in our universe) while strongly depressing equity indices and currencies; and (iv) there has been *no recovery*, despite material improvements in liquidity and declines in CTA participation since 2018.

**The self-fulfilling impact loop.** Before turning to the post-2008 break, it is useful to articulate what trend, viewed as a market mechanism rather than as a statistical anomaly, actually consists of. We adopt throughout this paper the view – developed precisely in the ETF context by Van der Beck et al. (2024), and foreshadowed by De Long et al. (1990) – that trend is chiefly (but most probably not only, see below) a self-fulfilling feedback loop:

*trend signals trigger directional trades, whose market impact reinforces the very price moves that produced the signal, which in turn sustains the signal for the next trader to act on.*

The profitability of trend and its very existence are thus two faces of the same coin: both depend on aggressive directional flow being absorbable by the market at reasonable cost, so that impact translates trade into price and price into renewed signal. Anything that breaks this loop – by raising execution costs to the point of disengagement, or by altering the relationship between

aggressive flow and price – should attack profitability and signal strength simultaneously. This is the lens through which we read the post-2008 evidence.

**Other mechanisms exist; the loop is not exclusive.** We do not claim that the self-fulfilling impact loop is the sole origin of trend. The behavioural-finance literature offers well-established alternatives – notably gradual incorporation of public news under underreaction (Hong and Stein, 1999; Daniel et al., 1998; Bouchaud et al., 2019), the slow diffusion of information across heterogeneously informed investors (Hong et al., 2000), and staggered accumulation by participants correctly anticipating a future event – each of which can produce price autocorrelation without invoking impact-mediated feedback. These mechanisms are not mutually exclusive with the loop; they plausibly coexist, with information-diffusion channels seeding trends and the impact loop amplifying them. In fact, we have direct empirical evidence in our data that some traders did anticipate large market moves and create trends accordingly, and that this channel has itself decayed around approximately the same period – see Appendix D, Fig. 18. The empirical observations we report below are therefore most naturally read as evidence that *both* the impact-loop and the anticipatory-trading components have been weakened in the post-2008 period, with the loop component decaying most visibly on small-tick contracts. We adopt the loop as our organising lens because it makes the cleanest predictions about the cross-section we study, not because we believe it is the only mechanism at work.

**Plan of attack.** This paper assesses four candidate explanations: (H1) capacity constraints; (H2) the electronication of futures markets; (H3) a structural shift in the interaction between CTA trades and aggregate order flow; and (H4) a microstructural mechanism whereby liquidity offered to trend followers has dried up. We reject H1–H3 on the grounds of timing, magnitude, or cross-sectional heterogeneity. Our central contribution concerns H4: the relevant cross-sectional variable separating degraded from surviving trend strategies is the *volatility-normalised tick size*. Partitioning the futures universe by this variable produces a clean dichotomy that no decomposition by asset class or liquidity replicates.

We propose a mechanism rooted in the post-crisis transition to HFT-dominated market making, whose liquidity-withdrawal behaviour in front of predictable directional flow has markedly different consequences for sparse (small-tick) and dense (large-tick) order books. Combined with the self-fulfilling loop above, this mechanism predicts – and the data confirm – that the small-tick collapse is not merely a story of higher transaction costs eating into PnL, but of the impact-mediated reinforcement of trends having been severed on those contracts. A complementary price-impact analysis shows that passive execution offers no escape: it forfeits the self-reinforcement channel while incurring adverse book-impact.

The paper is organised as follows. Sec. 2 defines the trend signals, portfolios, and CTA proxy. Sec. 3 documents the empirical decay across speed and asset class. Sec. 4 assesses H1–H3. Sec. 5 establishes tick size as the relevant cross-sectional variable. Sec. 6 develops the microstructural mechanism, including the role of price impact and the self-fulfilling loop. Sec. 7 concludes. Further supplements and details are provided in various appendices.

## 2 Trend Portfolios and a CTA Industry Proxy

We work with a cross-section of approximately 100 of the most liquid futures contracts, sampled at daily settlement, spanning four sectors: commodities (CMD), equity indices (IDX), currencies (FXR), and government bonds/yields (YLD). The data catalogue is detailed in Appendix A.

**Signal definition.** For each contract  $i$  and trading day  $t$ , the unnormalised trend signal on time scale  $\tau$  is the difference between a fast and a four-times slower exponentially weighted

moving average (EWMA) of close prices,  $\tilde{s}_i^\tau(t) = \langle p_i(t-1) \rangle_\tau - \langle p_i(t-1) \rangle_{4\tau}$ . Normalising by a slow estimate of its own dispersion yields the dimensionless signal

$$s_i^\tau(t) = \frac{\tilde{s}_i^\tau(t)}{\langle \langle \tilde{s}_i^\tau(t) \rangle \rangle_{16\tau}}, \quad (1)$$

which is comparable across contracts. Here  $\langle \cdot \rangle_\tau$  refers to the backward-looking EWMA with characteristic decay time  $\tau$  (in days) and  $\langle \langle \cdot \rangle \rangle_\tau$  refers to an exponentially weighted moving standard deviation (EWMSTD). We refer to a signal with parameter  $\tau$  as EWM- $\tau$ - $4\tau$ . As is industry practice, signals are clipped at  $\pm 2$  standard deviations:  $s_i^\tau(t) \mapsto \text{clip}(s_i^\tau(t), -2, 2)$ .

**Portfolio construction.** Two volatility-scaled portfolios constructed from all contracts are:

**Type 1 (equal-risk):** the position is volatility-normalised,

$$\pi_i^\tau(t) = \frac{s_i^\tau(t)}{\sigma_i(t)}. \quad (2)$$

**Type 2 (liquidity-weighted):** the position is normalised by its own volatility and by its liquidity expressed as a ratio of the aggregate liquidity in the portfolio,

$$\pi_i^\tau(t) = \frac{s_i^\tau(t) l_i(t)}{\sigma_i(t) L(t)}. \quad (3)$$

The volatility is defined as  $\sigma_i(t) = \langle |p_i(t-1) - p_i(t-2)| \rangle_{16\tau}$ ;  $l_i(t) = \langle V_i^{\text{w/o imp}}(t-1) \sigma_i(t) \rangle_{250}$  is a contract's liquidity, and  $L(t) = \sum_i l_i(t)$  is the aggregate portfolio liquidity, where  $V_i^{\text{w/o imp}}$  is the traded volume in contract  $i$  without implied trades. On each trading day the position is updated with the trade  $\Delta\pi_i^\tau(t) = \pi_i^\tau(t) - \pi_i^\tau(t-1)$  per product. The volatility normalisation ensures that each contract contributes a similar dollar-risk to the overall portfolio, while the liquidity-weighting becomes essential when scaling up to (CTA) industry size, since illiquid products cannot be scaled up in the same way as very liquid ones owing to differing price-impact costs.

**CTA proxy.** To match the risk of the aggregate CTA industry, the liquidity-weighted portfolio is rescaled according to industry-wide AUM  $S^{\text{CTA}}(t)$  from BarclayHedge (2025) at an annualised risk of  $r_a \approx 12\%$  (inferred from the SG CTA index):

$$\pi_i^{\text{CTA},\tau}(t) = \pi_i^\tau(t) \frac{S^{\text{CTA}}(t)}{\$1} \frac{r_a}{\sqrt{252}}. \quad (4)$$

Computing the resulting daily participation rate  $\text{PR}_i = |\Delta\pi_i^{\text{CTA}}| / V_i^{\text{w/o imp}}$  across contracts gives a cross-sectional median of  $\sim 0.9\%$ , broadly consistent with independent estimates by Quantica Capital (2022) and Lorenzen et al. (2025): the CTA industry represents less than 1% of the exchanged volume on futures. This agreement provides external validation of the proxy in Eq. (4).

### 3 Empirical Decay of Trend PnL

Equipped with the trend portfolios and the CTA proxy of Sec. 2, we now document the post-2008 performance break empirically. Three features emerge that any viable explanation must accommodate: an abrupt aggregate decay from 2008/9 onward, a strong dependence on signal speed (with fast trends most affected), and a marked heterogeneity across asset classes. Each is the subject of a dedicated subsection below. We present these patterns descriptively here; their mechanistic interpretation, and in particular the role of the self-fulfilling impact loop, is deferred to Sec. 6.

### 3.1 Aggregate cumulative PnL

Fig. 2 (left) shows the cumulative PnL of a fast trend portfolio (EWM-5-20) from 1950 to 2025. Two features stand out: the cumulative PnL is essentially flat from 2009 onward, although a weakening may already be detected from approximately 2000. The five-year rolling Sharpe ratio (right) collapses from a historical range of 1–2.5 to a level statistically indistinguishable from zero post-2010. This was also reported in Lempérière et al. (2014), and more recently by Schmidhuber (2021).

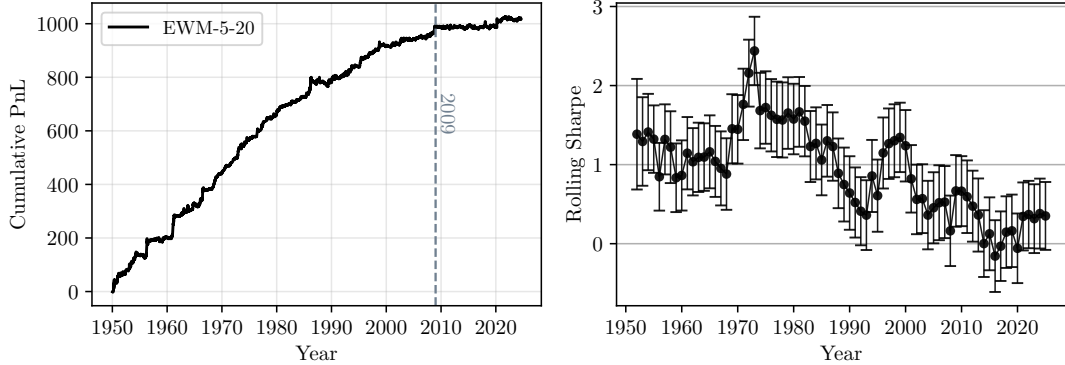


Figure 2: Left: cumulative PnL of EWM-5-20, 1950–2025. Right: corresponding 5-year rolling annualised Sharpe with bootstrap standard errors.

### 3.2 Speed dependence

Repeating the analysis for  $\tau \in \{5, 10, 20, 50\}$  reveals a striking asymmetry (Table 1 and Fig. 3): pre-2009 Sharpes are monotonically decreasing in  $\tau$  (from 0.84 at  $\tau=5$  to 0.70 at  $\tau=50$ ), whereas post-2008 the ordering reverses, with the fastest signal collapsing to 0.12 and the slowest still delivering 0.40.

$\tau$	Sharpe 1995–2009	Sharpe 2009–2025
5	$0.84 \pm 0.27$	$0.12 \pm 0.24$
10	$0.83 \pm 0.27$	$0.22 \pm 0.24$
20	$0.79 \pm 0.27$	$0.27 \pm 0.26$
50	$0.70 \pm 0.27$	$0.40 \pm 0.26$

Table 1: Sharpe ratios of EWM- $\tau$ - $4\tau$  trend signals over two sub-periods straddling the performance break. See also Fig. 3.

### 3.3 Asset-class heterogeneity

Fig. 4 disaggregates the cumulative PnL by sector. Trend has effectively vanished for IDX and FXR, while YLD and CMD show no appreciable degradation. As we will see in Sec. 5, this asset-class heterogeneity is most cleanly understood as a downstream consequence of a deeper microstructural variable.

## 4 Assessing Capacity, Electronification, and Order Flow

Having documented the post-2008 break and its qualitative signatures, we now confront three of the most natural candidate explanations: capacity constraints (H1), the electronification of

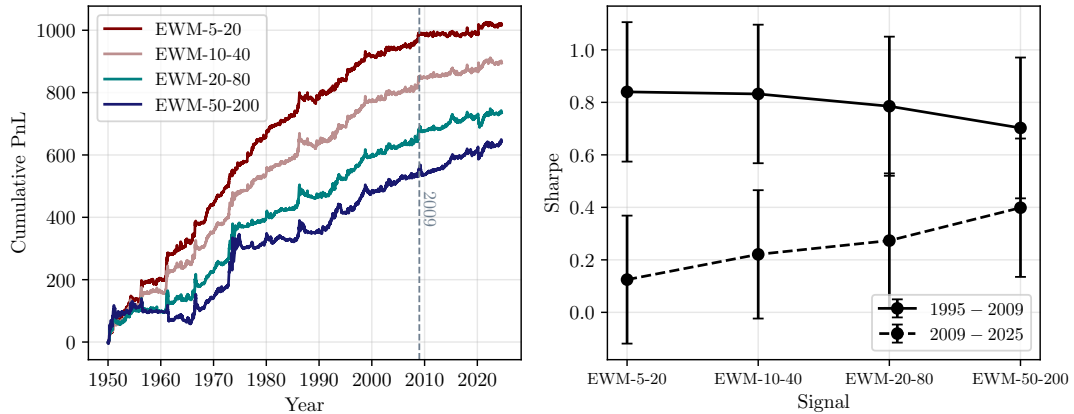


Figure 3: Left: cumulative PnL of EWM- $\tau$ - $4\tau$  portfolios for a range of fast scales  $\tau$ . Right: corresponding pre- and post-break Sharpe by signal. See also Table 1.

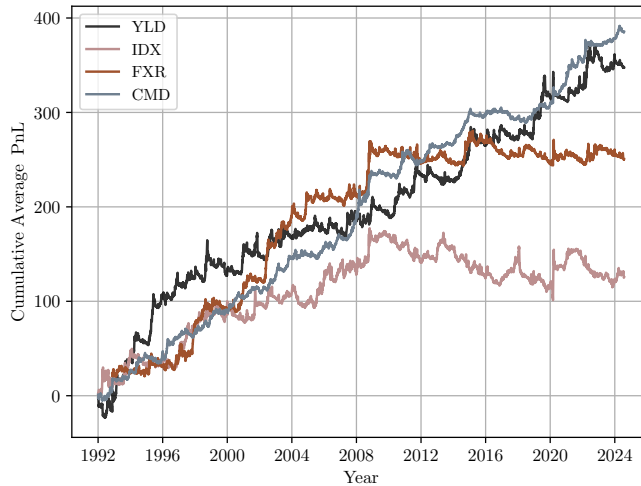


Figure 4: Cumulative PnL of a fast strategy (EWM-5-20), averaged within each asset class.

futures markets (H2), and a structural shift in the interaction between CTA trades and aggregate order flow (H3). For each, we ask whether the timing, the magnitude, and the cross-sectional pattern of the proposed channel match those of the observed PnL decay. We find that none does, although H3 will turn out to be a useful diagnostic when revisited at the right level of cross-section in Sec. 5.

#### 4.1 H1: Capacity constraints

The naive crowding argument – more capital arbitrages the signal away – is not viable for trend, since rational speculators in the presence of positive feedback should front-run rather than weaken trends (De Long et al., 1990). The relevant version is therefore the execution-cost story articulated by Quantica Capital (2025)<sup>1</sup> (see also Volpati et al. (2020)): under the

<sup>1</sup>Strictly speaking, Quantica Capital (2025) do not argue that trend has hit capacity industry-wide or that capacity constraints explain the post-2008 break. Their analysis is cross-sectional: at large AUM, risk allocation must concentrate in the most liquid commodities, eroding the diversification benefit that less liquid markets would otherwise contribute (they estimate 17% Sharpe drag at \$1B commodity capacity). They explicitly find no relationship between per-instrument Sharpe and liquidity after costs. We invoke their work here as the most carefully quantified version of the capacity hypothesis available, and as a useful motivator for our subsequent microstructural analysis, while acknowledging that capacity-driven erosion of diversification benefits in less liquid contracts may well be a genuine secondary effect operating alongside the mechanism we identify.

square-root impact law, total slippage scales as  $Q^{3/2}$  (see, e.g., Tóth et al. (2011); Bouchaud et al. (2018)), and beyond some position size  $Q$  net Sharpe collapses. We find this hypothesis problematic on four grounds.

*First, reverse causality.* CTA AUM (Fig. 5) grew through the 2000s, plateaued around 2012, and peaked in 2022 – several years *after* trend PnL went flat. The temporal ordering is the opposite of what the capacity story predicts.

*Second, no post-2018 recovery.* While CTA AUM stagnated after 2012, futures liquidity rose sharply from 2018 onward (see Fig. 5, right), mechanically reducing participation rates. Despite this, trend PnL did not recover. Crowding-driven decay typically exhibits a recovery signature once excess positions unwind (Mitchell and Pulvino, 2012); trend shows none.

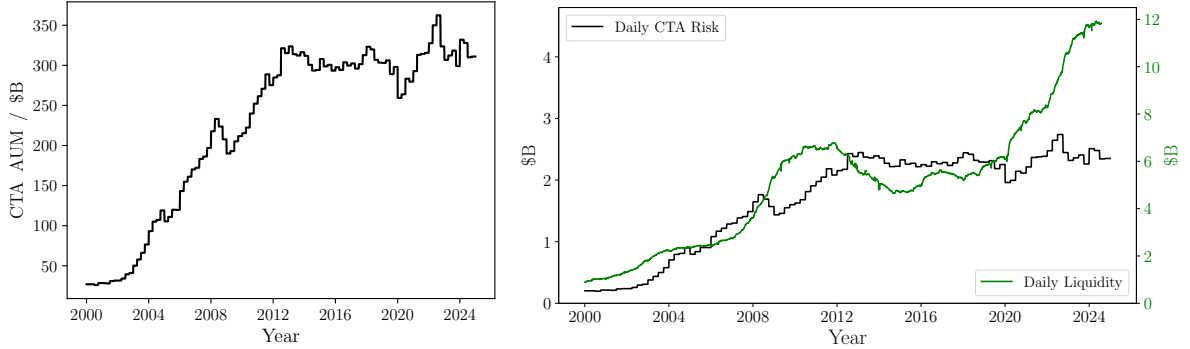


Figure 5: Left: estimated CTA industry AUM, 2000–2025 (BarclayHedge, 2025). Right: daily dollar risk of the CTA industry at  $r_a = 12\%$  (black, left axis) and aggregate daily liquidity (green, right axis).

*Third, the implied drag is too small.* A standard square-root impact calculation (Appendix B) at a 1% participation rate and  $\sim 9\%$  daily turnover yields an annualised Sharpe drag of roughly 0.1. This is non-trivial but still too small to explain the observed collapse from  $\sim 0.7$  to  $\sim 0$ , even when allowing for a factor-three error margin due to model uncertainty.

*Fourth (and most telling), signal degradation under zero-lag execution.* Recomputing the PnL with positions executed at the same day’s close (Fig. 6) – mechanically eliminating one full day of impact – produces equally flat post-2008 returns, even without costs. If capacity were the cause, removing execution costs should restore profitability, which it does not. This means the signal itself has degraded, rather than the strategy simply having become too costly to trade. As we will see, this fourth observation is particularly telling: it is the first hint that what has decayed is not merely the harvest but the underlying signal – exactly what the self-fulfilling loop framework predicts when the loop is broken.

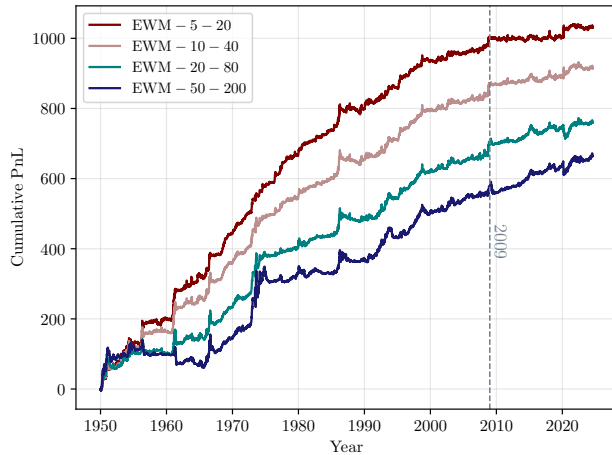


Figure 6: Cumulative PnL with zero-lag execution: positions identified on day  $t$  are executed at the day- $t$  close. Fast-signal performance (red, rosy) still remains flat post-2008.

## 4.2 H2: Electronification

The transition to electronic order books on major futures exchanges is sometimes invoked as a cause. Three observations from Fig. 7, which shows the fraction of electronically executed futures volume per sector on CME (Globex), cast doubt on that story: electronification was *gradual*, while the PnL break is abrupt; its sectoral *timing* does not align with the PnL break (equities electronified more than five years before the break, FX about contemporaneously); and its sectoral *ordering* does not match the PnL response (interest-rate futures electronified early but did not degrade). Although market electronification is a necessary precondition for the mechanism we propose below – it concentrates flow into a single visible book – it is not by itself the cause.

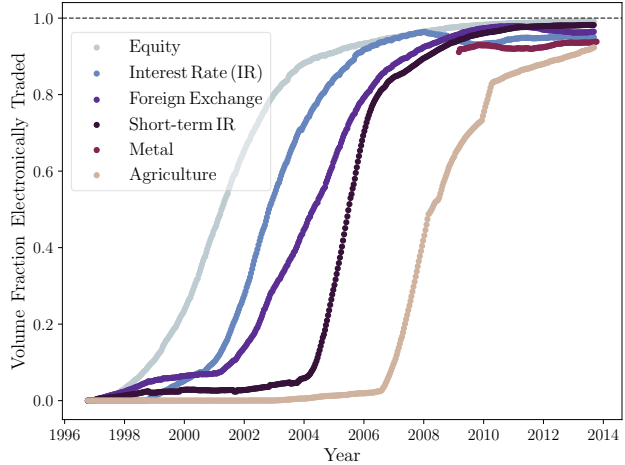


Figure 7: Progression of the futures volume fraction by asset class that is traded electronically on Globex versus the total traded CME futures volume, which includes pit trading through open outcry. Data courtesy of Robert Almgren, Quantitative Brokers.

## 4.3 H3: Order-flow interactions

Following Volpati et al. (2020), we define daily book and trade imbalances on volume-weighted 5-minute bars:

$$I_{i,t}^{\text{book}} = \frac{1}{V_{i,t}} \sum_{s \in t} \frac{V_{i,s}^{\text{bid}} - V_{i,s}^{\text{ask}}}{V_{i,s}^{\text{bid}} + V_{i,s}^{\text{ask}}} V_{i,s}, \quad I_{i,t}^{\text{trade}} = \frac{1}{V_{i,t}} \sum_{s \in t} \frac{V_{i,s}^{\text{BIV}} - V_{i,s}^{\text{SIV}}}{V_{i,s}^{\text{BIV}} + V_{i,s}^{\text{SIV}}} V_{i,s}, \quad (5)$$

where  $V_{i,s}$  is the volume traded in product  $i$  in each of the 5-minute time windows in a trading day, and  $V_{i,t}$  is the total traded volume of contract  $i$  in day  $t$ .  $V^{\text{bid/ask}}$  is a snapshot of the volume at the best bid/ask at the end of each bar window, and  $V^{\text{BIV/SIV}}$  is the cumulative buyer/seller-initiated volume per interval. The volume-weighting ensures that the daily statistics are dominated by liquid trading hours and not diluted by overnight futures trading.

The idea is to study the correlation between these flow indicators  $I$  and the expected change of position of trend followers,  $\Delta\pi^{\text{CTA}}$ , in order to detect possible changes in the way trend followers trade and, symmetrically, in the liquidity offered to them.

Aggregated across all futures markets, the correlation between  $\Delta\pi^{\text{CTA}}$  and book imbalance  $I^{\text{book}}$  has abruptly changed sign around 2010, especially for short-term trends (5–20 days), while showing essentially no change for long-term trends (Fig. 8, left). This is striking because it precisely parallels the change in PnL of short trends reported above, and motivates our initial working hypothesis. Indeed,  $\text{Corr}(\Delta\pi^{\text{CTA}}, I^{\text{book}})$  was negative before 2010 and positive after. In other words, the order book was thicker on the opposite side of the trend trade before 2010, meaning that liquidity was provided to trend followers during that period. Since then, liquidity has been more abundant for trades opposing the trend, which may indicate that either liquidity providers shy away from trading with trend followers, or that trend followers themselves use more limit orders to execute – or both.

The correlation with trade imbalance,  $\text{Corr}(\Delta\pi^{\text{CTA}}, I^{\text{trade}})$ , on the other hand, does not show any particular feature around 2010, but does change sign abruptly in 2015, suggesting that “anti-trend” (i.e. mean-reversion) trades have become dominant in the recent period, striking another blow to trend-following performance.

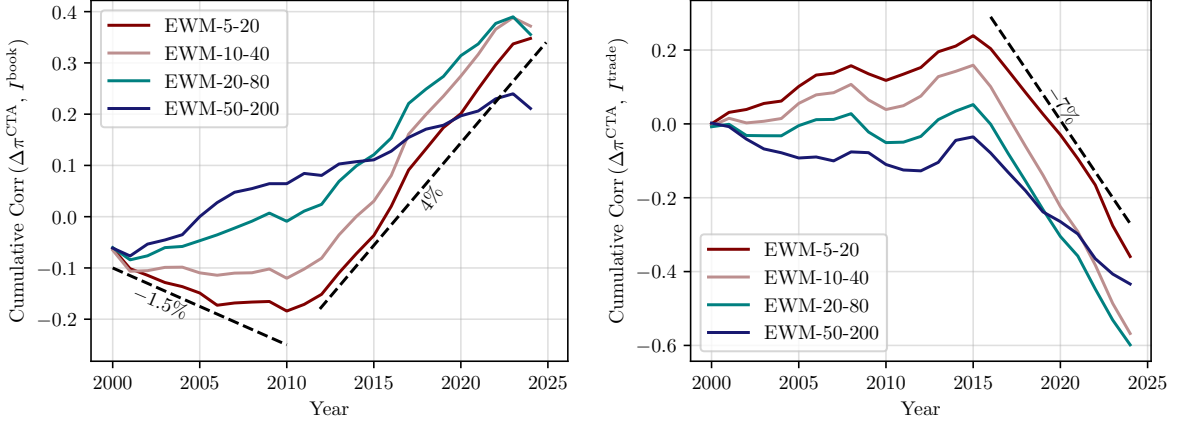


Figure 8: Annual cumulated correlations of trades  $\Delta\pi^{\text{CTA},\tau}$  with book imbalances (left) and with trade imbalances (right), averaged over the entire portfolios built from different signals EWM- $\tau$ - $4\tau$ . Dashed lines are for guidance.

Although suggestive, this hypothesis fails the cross-sectional test. Disaggregating by asset class, as shown in Fig. 9, reveals decisive mismatches between correlation changes and PnL outcomes (see Fig. 4):

1. Commodities undergo a sharp book-imbalance regime change but exhibit *no* PnL degradation whatsoever; currencies show a similar change in correlation structure and the post-2010 PnL is flat.
2. Yields show essentially no correlation change and equally show no PnL degradation.
3. Indices show a reverse pattern but a similar trend degradation.
4. The post-2010 sign is common across YLD, CMD, and FXR but their PnL outcomes differ entirely.

No monotonic mapping exists between the correlation changes and the PnL outcomes at the asset-class level. An intra-day volume-clock decomposition (Appendix C) reveals that the first 20% of daily volume behaves systematically differently from the rest – consistent with morning-concentrated CTA execution – but does not resolve the cross-sectional inconsistency.

H3 is therefore insufficient at the asset-class level of decomposition. The diagnostic itself, however, will re-emerge usefully at a different level of cross-section under H4.

## 5 Tick Size as a Discriminant Factor

We now establish the central empirical result of the paper: the relevant cross-sectional variable separating degraded from surviving trend strategies is the *volatility-normalised tick size*.

### 5.1 Tiering procedure

For each product  $i$  and month  $m$ , define the average tick-to-volatility ratio

$$\bar{\rho}_{i,m} = \frac{1}{D_m} \sum_{t=1}^{D_m} \frac{\Psi_i(t)}{\sigma_i(t)}, \quad (6)$$

where  $\Psi_i$  is the tick size of the contract,  $\sigma_i$  is the daily volatility estimator of Sec. 2, and  $D_m$  is the number of trading days in month  $m$ . Each month, products are ranked in ascending order

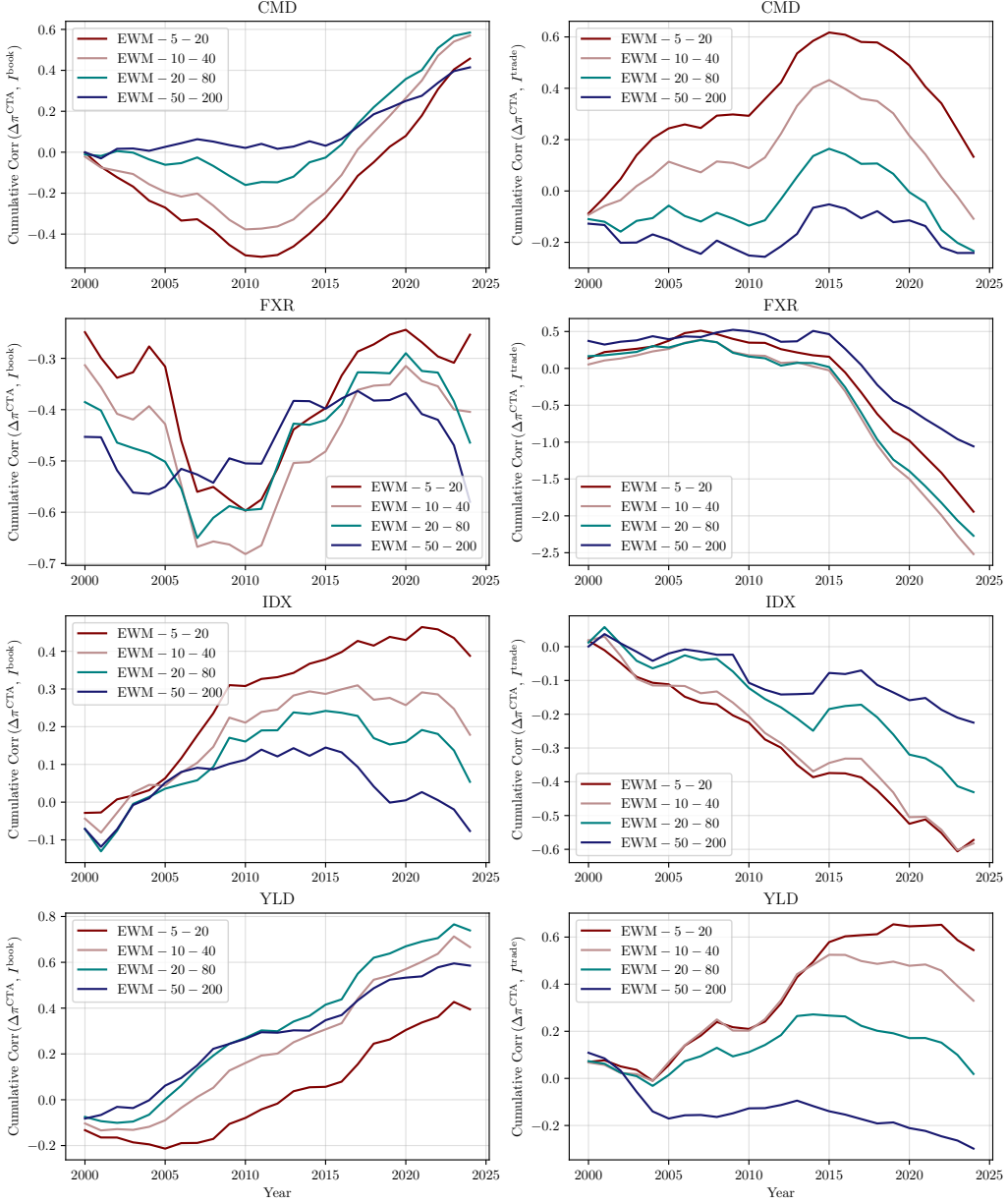


Figure 9: Same as Fig. 8 but averaged per asset class.

by  $\bar{\rho}_{i,m}$ ,

$$R_{i,m} := \text{rank}_{j \in \mathcal{P}_m}(\bar{\rho}_{j,m})[i] \in \{1, 2, \dots, N_m\}, \quad (7)$$

where  $\mathcal{P}_m$  denotes the set of  $N_m \equiv |\mathcal{P}_m|$  products, and partitioned into two equal-sized tiers:

$$\text{Tier}_{i,m} := \begin{cases} \text{small tick (ST)}, & \text{if } R_{i,m} \leq \lfloor N_m/2 \rfloor, \\ \text{large tick (LT)}, & \text{otherwise.} \end{cases} \quad (8)$$

A product is categorised as small (large) tick if its tick-to-volatility ratio is in the lowest (highest) 50%. The partition is used causally and recomputed monthly, so that a contract whose volatility regime or tick size changes can migrate between tiers. Effectively, however, products rarely migrate between tiers in our sample. Note that ST and LT refer to tick size, not to be confused with “short trends” or “long trends”.

## 5.2 Results

Fig. 10 shows the cumulative PnL of the equal-risk trend portfolio (Eq. (2), without liquidity weighting), causally conditioned on the monthly tick-size tier and disaggregated by signal horizon. The dichotomy is stark: short-trend PnL has *completely* degraded for small-tick contracts after 2008, uniformly across signal horizons EWM- $\tau$ - $4\tau$ , while the cumulative PnL of large-tick contracts is virtually unaffected by the break and continues to accrue at roughly the pre-2009 rate, even at the highest frequency. The result is preserved when the tick-size tiering is performed *within* each asset class rather than across the full universe (Appendix F), suggesting that the dependence of fast-trend degradation on volatility-normalised tick size is approximately monotonic rather than driven by a single threshold.

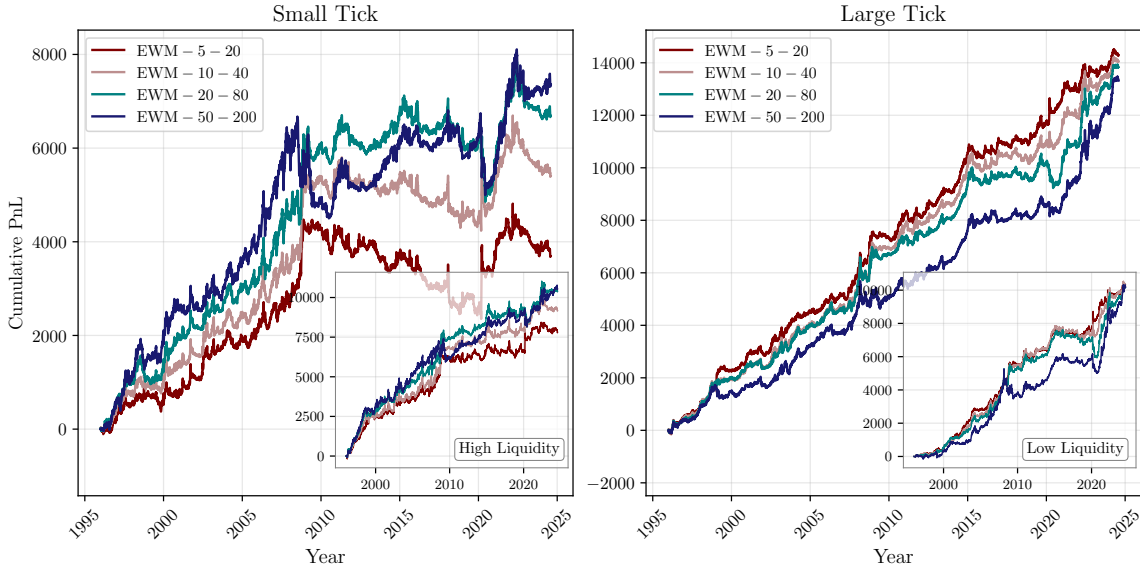


Figure 10: Cumulative trend PnL conditioned on the monthly tick-size tier. Left: small-tick contracts. Right: large-tick contracts. Equal-risk portfolio, no liquidity weighting (Eq. (2)). Insets: same, but filtered by equally-sized liquidity tiers instead of tick-size tiers.

Fig. 11 (top) quantifies the dichotomy. Pre-break Sharpes cluster around 0.8 for ST and 1.4 for LT for the equal-risk portfolio. Post-break, ST Sharpes collapse to essentially zero (mildly negative for the fastest signals), while LT Sharpes remain in the range 1.0–1.2. The relative degradation is  $\sim 100\%$  for ST and  $\sim 0\text{--}30\%$  for LT. Fig. 11 (bottom) repeats the analysis for the liquidity-weighted portfolio (Eq. (3)), from which qualitatively similar insights may be inferred – the finding holds with and without liquidity weighting. Beyond that, the comparison also shows that liquidity has a measurable but secondary effect on the PnL outcome.

**Classifying by liquidity does not work.** A natural concern is that liquidity might tier the cross-section equally well, since liquidity and tick size are negatively correlated (log-log Pearson correlation of  $-0.35 \pm 0.08$ ; see Appendix E). It is also anecdotally known that trends still work on lower-liquidity products. The result, however, is unambiguously negative: the decomposition by liquidity tier (Fig. 10, insets; see also Fig. 20 in Appendix E) does not dichotomise as cleanly. Liquidity-tiered PnLs are inconsistent across horizons: not all fast signals on liquid contracts have collapsed, and there is no clean ordering between the high- and low-liquidity sub-portfolios. *Tick size – rather than liquidity, asset class, or electrification – is the cross-sectional variable that best explains trend survival.* The asset-class heterogeneity documented earlier is, on this reading, a downstream symptom of the clustering of IDX and FXR in the small-tick tier and of YLD and most CMD in the large-tick tier.

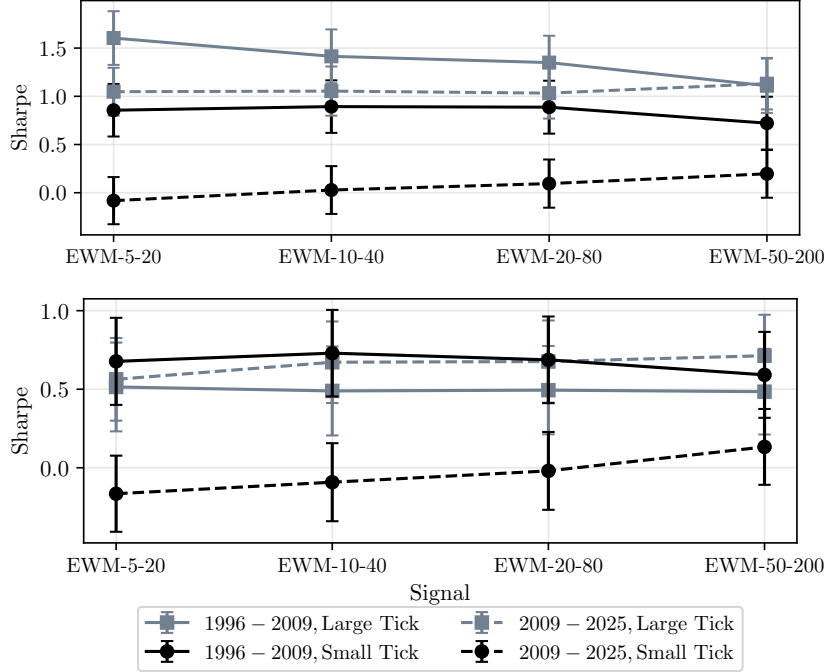


Figure 11: Sharpe ratios by tick-size tier and signal horizon, pre- and post-break. Top: equal-risk portfolio. Bottom: liquidity-weighted portfolio. Errors are bootstrap standard errors.

**Within-contract confirmation.** Two further decompositions confirm the framework. First, partitioning each contract’s days by volatility (per-contract per-year median, causal) shows that trends are generally more profitable in periods of low volatility – the *LeBaron effect* (LeBaron, 1992a,b). Interestingly, low-volatility periods on small-tick contracts continue to accrue PnL even after the overall PnL break: small-tick products in low-volatility regimes behave similarly to large-tick contracts – exactly as expected if the operative variable is  $\Psi/\sigma$  rather than  $\Psi$  alone. Second, partitioning by daily return magnitude shows that the trend break is a phenomenon of *large-return* days only: the PnL contribution from sub- $1\sigma$  days is essentially invariant to the post-2008 regime change across all horizons and tiers. The signal harvested on small returns has not decayed; what has been eliminated is specifically the trend follower’s ability to profit from large directional moves on small-tick contracts. Both decompositions are reported in detail in Appendix D and impose constraints that the mechanism developed below naturally satisfies.

## 6 HFT Liquidity, the Self-Fulfilling Loop, and the Sparse-vs.-Dense Asymmetry

We now turn to the mechanism. The organising idea is the self-fulfilling loop introduced in Sec. 1: trend exists, and remains profitable, because trend trades push prices in the direction of the signal, sustaining it for the next round of trend followers to act on. The loop has two preconditions. First, trend followers must be able to execute aggressively at a cost that does not exceed the impact-mediated alpha they thereby create. Second, the relationship between aggressive flow and price – the impact function – must remain intact, so that flow continues to translate into the price moves the signal needs.

We argue in this section that both preconditions held until roughly 2010 across the futures universe, and that since then both have been compromised on small-tick contracts and largely preserved on large-tick ones. The mechanism behind this asymmetry is the post-crisis transition to HFT-dominated market making, which operates in both tick-size tiers but has profoundly

different consequences depending on the geometry of the limit order book (LOB). The empirical signature of the broken loop, we will see, is twofold: a rotation of the LOB against trend execution (Sec. 6.1), and a flattening of the contemporaneous return-versus-book-imbalance relationship that quantifies the cost of providing depth in front of directional flow (Sec. 6.3). Together, these two changes are sufficient to explain why both the PnL and the signal itself have collapsed on small-tick contracts.

## 6.1 Liquidity provision against trend flow has rotated

We first revisit the order-flow diagnostics of Sec. 4 but disaggregated by tick-size tier rather than by asset class. The result is shown in Fig. 12. For slow signals, no material change in the correlations with  $I^{\text{book}}$  (left) is visible in either tier. For fast signals on *large-tick* contracts, the correlation  $\text{Corr}(\Delta\pi^{\text{CTA}}, I^{\text{book}})$  has changed sharply from  $\sim -3\%$  p.a. pre-2010 to  $\sim +4\%$  p.a. thereafter. To wit: pre-2010, on a fast trend buy day ( $\Delta\pi^{\text{CTA}} > 0$ ), the negative correlation implies  $V^{\text{ask}} > V^{\text{bid}}$  – there was more resting volume offered to trend followers than to mean-reverters; post-2010, the positive correlation implies  $V^{\text{ask}} < V^{\text{bid}}$  – the liquidity in the book has rotated *against* the trend follower.

For *small-tick* contracts, the correlation has been positive throughout, but its post-2010 magnitude on fast signals has grown materially: the small-tick LOB, never abundant in liquidity in the direction of trend, has become even more shallow.

The correlation with trade imbalance in Fig. 12 (right column) also shows a clear regime change, but only in 2015. This suggests either a change in the execution strategy of trend followers or more market-order execution from mean-reverters; in either case, this change is more a consequence than a cause of the demise of short trends from 2010 onwards.

## 6.2 The mechanism

The puzzle to be explained is therefore the following: post-2010, the LOB has rotated against fast trend execution across *both* tick-size tiers, yet the PnL consequences are sharply asymmetric – innocuous for large ticks and devastating for small ticks. We propose that the post-2010 break results from the combination of two ingredients.

**(i) A change in the liquidity-provision regime.** The post-2008 period coincides with the substantial completion of the transition from traditional bank-affiliated and proprietary-desk market making, operating on inventory horizons of hours to days, to high-frequency-trading

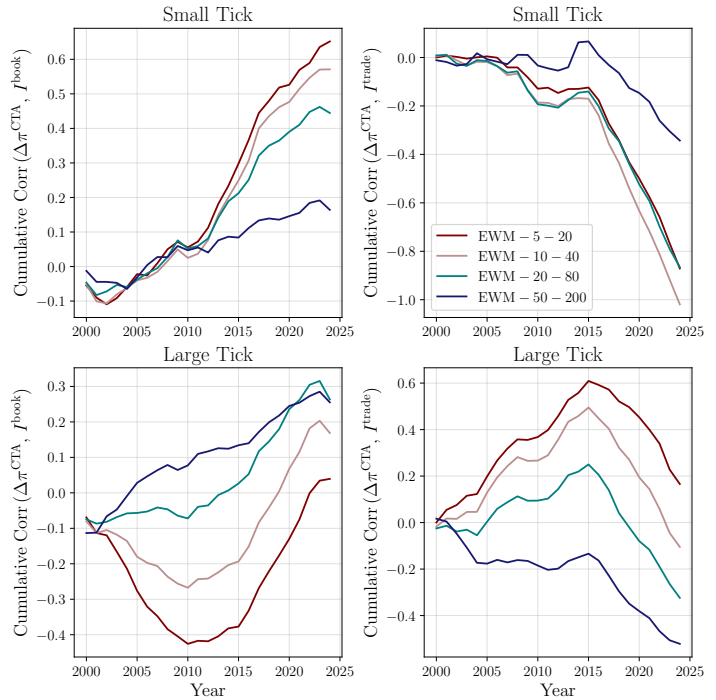


Figure 12: Cumulative annual-average correlation between CTA trades (Eq. 4, liquidity-weighted) and book imbalance (left) / trade imbalance (right). Top: small-tick tier. Bottom: large-tick tier.

market making on intraday flat-inventory mandates with extremely tight spread-capture economics (Kirilenko et al., 2017; Menkveld, 2013; Chaboud et al., 2014; Hendershott and Riordan, 2013). The HFT market-making business model is structurally incompatible with absorbing the predictable and persistent directional flow that aggregate CTA trading generates. The empirical literature documents that HFTs systematically *withdraw* liquidity in front of large institutional orders rather than supply it, and that execution costs for such orders are correspondingly elevated (Korajczyk and Murphy, 2019; Van Kervel and Menkveld, 2019). Whether the relevant change is one of *identity* (a new population of providers, who never absorbed such flow) or *behaviour* (incumbents tightening risk preferences after the 2008 inventory losses; see Adrian and Shin 2010) is immaterial for our argument; the evidence is consistent with both, plausibly in combination. The correlation changes reported in Fig. 12 (left column) indicate that LOB liquidity provision has rotated against trend followers, most probably as a consequence of this evolution of market-making practices.

**(ii) Structural differences between small- and large-tick LOBs.** Independent of any particular generation of market makers, small-tick LOBs are intrinsically *sparse*: gaining priority requires offering better prices, so expected gains are smaller relative to adverse-selection costs; equilibrium posted depth is therefore small, and gaps between filled price levels are common (Bouchaud et al., 2018; Dayri and Rosenbaum, 2015). Large-tick LOBs are intrinsically *dense*: the spread is meaningfully wider than what is needed to compensate for adverse selection, the queueing rent at the front of the queue is substantial, and resting volume builds up at multiple deep levels.

**Combined consequence: the loop holds on large ticks and breaks on small ticks.** The HFT-driven rotation of the book operates in both tiers (Fig. 12), but its consequence is asymmetric. In a sparse small-tick LOB, withdrawal removes the residual depth that previously allowed fast trend execution to proceed at reasonable cost – which is precisely what the self-fulfilling loop requires, since the CTA industry’s flow comes in large size. Trend followers would have had to “walk the book” to execute, incurring substantial transaction costs; this is the short transitory period before they acknowledged that liquidity previously available to them had significantly receded. The consequence, in our scenario, is that trend followers structurally disengaged from short-horizon trend in those products (Korajczyk and Murphy, 2019). Once they did so, the loop broke on its input side: the impact-mediated reinforcement of nascent trends disappeared along with the flow that produced it, and the small-tick *signal* – not just the harvest – decayed. This is exactly the pattern documented in Sec. 4 under zero-lag execution and corroborated by the within-contract decompositions of Sec. 5.

By contrast, on dense large-tick LOBs, residual depth at the best quotes and at deeper levels remains sufficient for execution to proceed largely unperturbed compared to the pre-2010 period. Trend followers continue to trade aggressively, the impact-mediated reinforcement continues to operate, and both the signal and the PnL remain intact. Fig. 13 sketches the sparse small-tick and dense large-tick LOBs respectively, and illustrates the asymmetric effect of liquidity withdrawal under a buy-trend.

This account is also consistent with the within-contract decompositions of Sec. 5 and Appendix D. The volatility decomposition is mechanically predicted: in low-volatility regimes,  $\Psi/\sigma$  rises and small-tick contracts behave microstructurally like larger-tick ones, so the loop continues to operate. The return-magnitude decomposition is also mechanically predicted: liquidity withdrawal is triggered by the size of detected directional flow, and the adverse-selection cost of providing liquidity is small for weak trend signals – hence depth does not recede significantly and small-move trend PnLs are mostly unaffected.

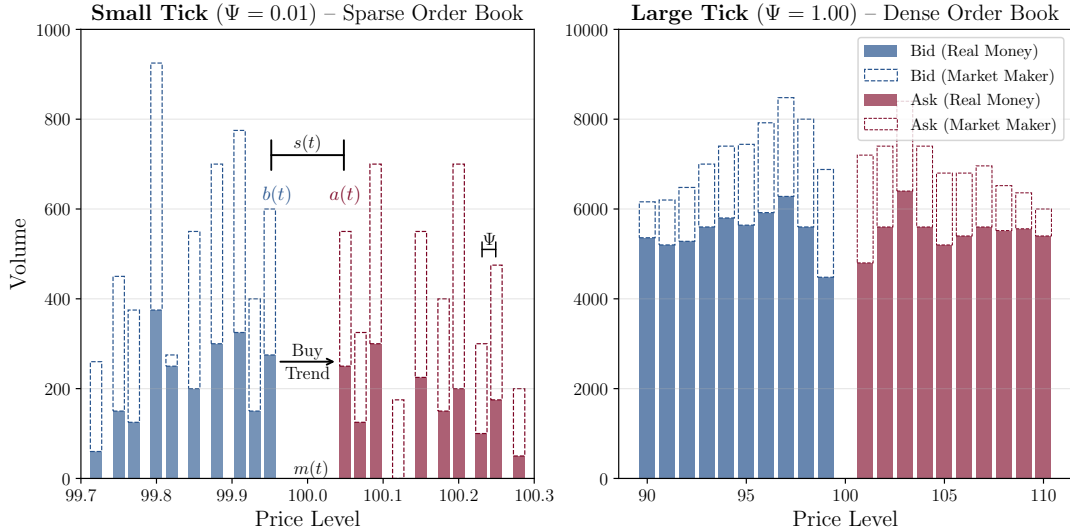


Figure 13: Limit order book sketches for a small-tick (left) and large-tick (right) asset. Dashed bars exemplify the liquidity provided by market makers, while solid bars subsume all other volume. The units  $[\Psi] = [\text{price level}]$  are arbitrary (futures) price units and can differ between contracts;  $a(t)$  and  $b(t)$  are the best ask and bid prices, which can move in units of the tick  $\Psi$ ;  $s(t) = a(t) - b(t)$  is the spread, and  $m(t) = \frac{a(t)+b(t)}{2}$  the mid-price. Note the difference in order of magnitude on the y-axes.

### 6.3 The role of price impact: the loop, made explicit

Sec. 6.2 argued that the degradation of not only the trend PnL but also the trend *signal* on small-tick contracts is a consequence of trend followers' retreat from those products. This is more than a casual claim: it is a direct prediction of the self-fulfilling loop articulated in Sec. 1. De Long et al. (1990) showed that trend signals are subject to positive feedback, so that more trend trading should reinforce, rather than crowd out, the signal. Van der Beck et al. (2024) have recently made this scenario very precise in the ETF context, quantifying the role of price impact; see also Patzelt and Bouchaud (2018) and Fig. 14 (right) for microstructural evidence. The right panel shows the contemporaneous relationship of normalised five-minute returns to the equal-bin trade imbalance: under a buy-trend for which statistically  $V^{\text{BIV}} > V^{\text{SIV}}$  and hence  $I^{\text{trade}} > 0$ , the return is on average positive, mechanically reinforcing the trend signal. This is the loop, observable.

The implication for our story is straightforward. If trend followers stopped trading aggressively on small-tick contracts, the positive impact channel that fed back into the signal weakened correspondingly: weak nascent trends could no longer be amplified into full-fledged ones, and the signal's autocorrelation – not just its harvest – decayed. On large-tick contracts, where aggressive execution remained viable, the loop continued to operate and the signal continued to exist.

Fig. 14 (left) sharpens the picture by showing the relationship between the five-minute normalised return and its equal-bin *book* imbalance. It reveals striking differences between small ticks and large ticks, and – more importantly – between small ticks before and from 2011, while the return-versus-trade-imbalance relation (right panel) is stable over time and qualitatively similar across tiers.

What do the small-tick curves tell us? Before 2011, there is clear adverse selection: liquidity imbalance between bid and ask is negatively correlated with the return. Limit orders at the bid are likely to be executed at a higher price than the bar's close, and vice versa, so liquidity providers face net inventory losses. The average adverse selection reaches a maximum at

intermediate book imbalances ( $I^{\text{book}} \approx 0.1$ ; see Fig. 14 (left, red)). Since 2011, however, this effect has nearly entirely disappeared – the correlation is close to zero (dashed red line). This observation supports our hypothesis that liquidity providers (in particular HFTs) in small-tick futures have become largely immune to adverse selection, or at least considerably more wary of it than in the past. The mechanical signature of liquidity withdrawal is precisely this flattening: depth that would previously have been “run over” by aggressive trend flow no longer rests long enough to appear in the imbalance statistics. The cost has not disappeared; it has migrated from the market maker’s inventory to the trend follower’s slippage.

The correlation is persistently negative for large ticks, which is expected to some extent: market-maker profits on large spreads can remain positive even when partly eaten up by adverse selection.

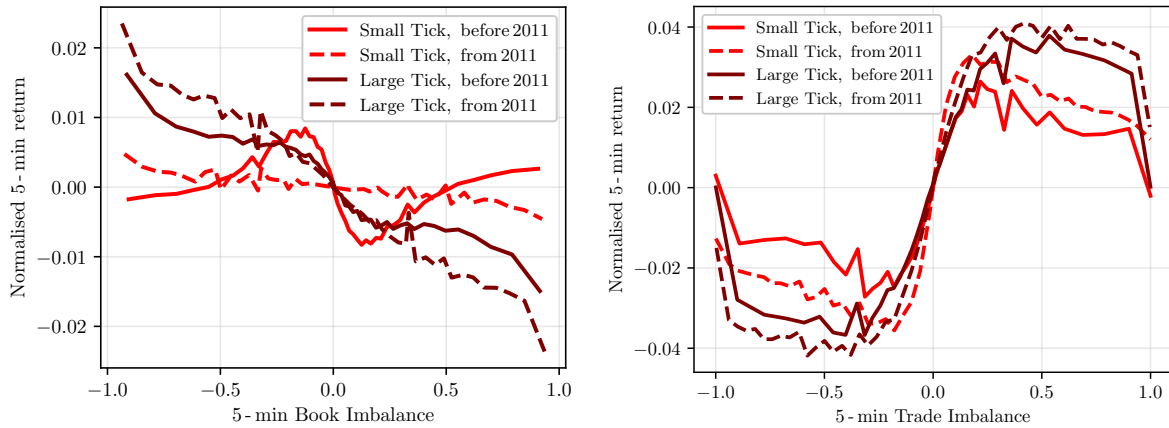


Figure 14: Normalised 5-minute returns as a function of contemporaneous book imbalance (left) and trade imbalance (right), for small-tick (red) and large-tick (maroon) contracts, before (solid) and from (dashed) 2011. The x-axis is quantile-binned.

#### 6.4 Limit orders are no remedy: missed opportunities and a broken loop

Can fast trend followers circumvent the small-tick constraint by switching from market-order to limit-order execution? We believe not, for two distinct but mutually reinforcing reasons, both visible in the empirical price-impact relationships of Fig. 14.

##### (a) Trend limit orders are penalised by missed opportunities, not adverse selection.

A trend follower posting a passive bid in order to buy faces the risk of not being executed if their prediction is realized, leading to an increased execution price if the decision is not executed quickly. The dominant cost of passive execution for a trend follower is therefore not adverse selection in the usual sense (being filled by better-informed counterparties before the price moves against them); it is the opposite – the *missed-opportunity cost* of failing to be filled while the price runs away in the direction of the signal. The very fact that the signal is informative about the next move guarantees that the follower’s passive bid will be filled preferentially in the bad states of the world (when the price drops through it) and missed in the good ones (when the price runs away upward). Limit-order execution therefore does not save costs; it re-labels them, replacing visible slippage with invisible opportunity loss. More generally, limit order execution is favoured in mean-reverting environments, and detrimental in trend following environments (see e.g. Bouchaud et al. (2018), chapter 17).

**(b) Passive execution forfeits the self-fulfilling loop.** The deeper problem is that even a costlessly executed limit order would not solve the trend follower’s predicament, because passive

trades do not feed the self-reinforcing impact channel that sustains the signal in the first place. The trade-imbalance impact of Fig. 14 (right) is generated by *aggressive* flow: it is the buyer-initiated volume that pushes prices up, not the resting bid that sits and waits. A trend follower who replaces market orders with limit orders ceases to contribute to  $I^{\text{trade}}$  in the direction of the trend, and – by exactly the mechanism formalised in Sec. 6.3 – no longer participates in the impact-mediated reinforcement of the very price moves they are trying to exploit. The loop, on which trend depends both for its profitability and for its existence, is broken from the trend follower’s side.

Taken together, (a) and (b) leave no execution style that side-steps the post-2008 microstructural change on small-tick contracts. Aggressive execution is constrained by the thinness of the post-withdrawal small-tick book; passive execution incurs missed-opportunity costs that scale with the very informativeness of the signal, and forfeits the impact channel that makes the signal worth trading in the first place. This is, in our view, the fundamental reason why the small-tick break has proven structural: it is not an artefact of any particular implementation choice, but a consequence of the relationship between aggressive flow and price formation on which trend itself depends.

## 7 Discussion and Conclusion

The post-2008 decay of trend-following returns has been one of the most discussed – and least understood – regularities in the recent history of systematic investing (see e.g. Lempérière et al. (2014); Schmidhuber (2021); Quantica Capital (2025)). We have argued that, at root, it is neither a flow phenomenon, nor a capacity phenomenon, nor a consequence of electronification per se, but a microstructural one. The volatility-normalised tick size cleanly partitions the futures universe into a small-tick subset on which fast trend has collapsed and a large-tick subset on which it has remained essentially intact. No decomposition by asset class, liquidity, or sectoral electronification date reproduces this dichotomy.

The interpretive frame we propose takes the self-fulfilling impact loop – signal  $\rightarrow$  trade  $\rightarrow$  impact  $\rightarrow$  reinforced signal – as the mechanism through which trend exists in the first place. Trend followers do not merely harvest a pre-existing anomaly: their aggressive directional flow, mediated by impact, sustains the very price patterns they trade on. The loop has two preconditions: that aggressive execution be feasible at reasonable cost, and that the relationship between aggressive flow and price remain intact. Both held until roughly 2010 across the futures universe; since then, both have been compromised on small-tick contracts and preserved on large-tick ones.

The mechanism behind this asymmetry is the post-2008 transition to HFT-dominated market making, which replaced a generation of inventory-tolerant liquidity providers with one whose business model is structurally incompatible with absorbing predictable directional flow. The resulting liquidity withdrawal in front of CTA orders operates in both tick-size tiers, but its consequences are asymmetric. On dense large-tick books, residual depth at the best quotes and at deeper levels remains sufficient for execution to proceed largely unperturbed; the loop continues to turn, and both the signal and the PnL survive. On sparse small-tick books, withdrawal removes the residual depth that previously supported fast trend execution, forcing trend followers either to “walk the book” aggressively or to retreat from the contract altogether. As they retreated, the loop broke on its input side: the impact-mediated reinforcement of nascent trends disappeared along with the flow that produced it. The collapse of the small-tick trend signal under zero-lag execution – for which execution costs is not an issue – is the cleanest empirical fingerprint of this broken loop. The within-contract decompositions by volatility and by return magnitude confirm that the operative variable is  $\Psi/\sigma$  rather than  $\Psi$  alone, and that

the break activates precisely on the large directional moves that would, under the old regime, have triggered absorption by inventory-tolerant market makers.

The contemporaneous return-versus-book-imbalance relationship makes the same story visible at intraday frequency. Its pre-2011 small-tick negative steepness measures the cost of providing depth in front of directional flow – exactly the cost the previous generation of market makers were absorbing. Its post-2011 flattening is the mechanical signature of liquidity withdrawal: depth that would have been run over no longer rests long enough to appear in the imbalance statistics.

Some practical implications follow. The break is structural; we see no plausible scenario in which it reverts absent a corresponding structural change in liquidity provision – whether through regulation, the entry of a new class of inventory-tolerant intermediaries, or a re-tariffing of market-making rents. Switching from aggressive to passive execution is not an option: passive execution incurs opportunity costs and forfeits the self-reinforcement channel that sustains the signal. Capacity estimation for trend portfolios should accordingly be carried out at the tick-size-tier level rather than at the asset-class level; aggregate participation rates can be substantially below historical bounds while still being binding within the small-tick subset.

Several questions remain open. Direct tests of the mechanism using HFT inventory data around large CTA rebalancing events would sharpen the causal claim and quantify the speed at which depth is withdrawn and refilled. The possibility of recovering trend in microstructural niches – contracts below the HFT participation threshold, venues with different market-maker mandates, or markets where tick-size regimes have shifted – is an empirical question we leave to future work. So is the symmetric one: whether the same mechanism disadvantages other systematic strategies that generate predictable directional institutional flow, and whether, conversely, strategies that trade against such flow have benefited from a complementary tailwind.

A more fundamental open question concerns the relative weight of the self-fulfilling impact loop among the mechanisms that generate trend in the first place. The literature has long offered alternatives that do not rely on impact-mediated reinforcement: gradual incorporation of public news under behavioural underreaction (Hong and Stein, 1999; Daniel et al., 1998; Bouchaud et al., 2019); slow, staggered execution by informed participants who correctly anticipate a future event and accumulate positions ahead of it; and the gradual diffusion of private information through a heterogeneously-informed investor base (Hong et al., 2000). These mechanisms are not mutually exclusive with the loop we emphasise; on the contrary, they plausibly coexist, with the loop amplifying trends that have an exogenous origin and the impact channel translating slowly arriving information into prices. Our reading of the post-2008 evidence is that the impact-loop component has been disproportionately weakened on small-tick contracts – which is consistent with the near-total collapse of fast trends there – while the information-diffusion component, operating on slower horizons, remains largely intact, consistent with the partial survival of slow trends across the universe. Disentangling these contributions quantitatively, ideally by exploiting cross-sectional or cross-venue variation in the strength of the impact channel, strikes us as a particularly worthwhile direction for future work. In fact, we do have direct empirical evidence some traders did anticipate large market moves and created trends accordingly, and that this possibility has decayed around approximately the same period, see Fig. 18 of Appendix D.

Finally, our analysis suggests that the joint design of tick size and market-maker obligations has first-order consequences for the persistence of medium-frequency anomalies sustained, in part, by self-fulfilling impact loops; this is a topic on which the regulatory and academic literature have arguably underweighted the perspective of the directional taker of liquidity.

## Acknowledgements

We thank Adam A. Majewski for facilitating the access to bar data and for fruitful discussions. Further, we are grateful to Société Générale Prime Services & Clearing for providing the SG CTA Index data, and to Robert Almgren (Quantitative Brokers) for the electronification data and helpful discussions.

## References

- T. Adrian and H. S. Shin. The changing nature of financial intermediation and the financial crisis of 2007–2009. *Annu. Rev. Econ.*, 2(1):603–618, 2010.
- N. Baltas and R. Kosowski. Momentum strategies in futures markets and trend-following funds. *Available at SSRN 1968996*, 2013.
- BarclayHedge. CTA Industry Assets Under Management, 2025. URL <https://ionanalytics.com/barclayhedge/solutions/assets-under-management/cta-industry-assets-under-management/>. Data accessed on 20.07.2025.
- V. Bogousslavsky. Infrequent rebalancing, return autocorrelation, and seasonality. *The Journal of Finance*, 71(6):2967–3006, 2016.
- J.-P. Bouchaud, J. Bonart, J. Donier, and M. Gould. *Trades, quotes and prices: financial markets under the microscope*. Cambridge University Press, 2018.
- J.-P. Bouchaud, P. Krueger, A. Landier, and D. Thesmar. Sticky expectations and the profitability anomaly. *The Journal of Finance*, 74(2):639–674, 2019.
- A. P. Chaboud, B. Chiquoine, E. Hjalmarsson, and C. Vega. Rise of the machines: Algorithmic trading in the foreign exchange market. *The Journal of Finance*, 69(5):2045–2084, 2014.
- K. Daniel, D. Hirshleifer, and A. Subrahmanyam. Investor psychology and security market under-and overreactions. *The Journal of Finance*, 53(6):1839–1885, 1998.
- K. Dayri and M. Rosenbaum. Large tick assets: implicit spread and optimal tick size. *Market Microstructure and Liquidity*, 1(01):1550003, 2015.
- J. B. De Long, A. Shleifer, L. H. Summers, and R. J. Waldmann. Positive feedback investment strategies and destabilizing rational speculation. *The Journal of Finance*, 45(2):379–395, 1990.
- E. F. Fama. Efficient capital markets. *Journal of finance*, 25(2):383–417, 1970.
- T. Hendershott and R. Riordan. Algorithmic trading and the market for liquidity. *Journal of financial and quantitative analysis*, 48(4):1001–1024, 2013.
- S. L. Heston, R. A. Korajczyk, and R. Sadka. Intraday patterns in the cross-section of stock returns. *The Journal of Finance*, 65(4):1369–1407, 2010.
- H. Hong and J. C. Stein. A unified theory of underreaction, momentum trading, and overreaction in asset markets. *The Journal of finance*, 54(6):2143–2184, 1999.
- H. Hong, T. Lim, and J. C. Stein. Bad news travels slowly: Size, analyst coverage, and the profitability of momentum strategies. *The Journal of finance*, 55(1):265–295, 2000.
- B. Hurst, Y. H. Ooi, and L. H. Pedersen. A century of evidence on trend-following investing. *The Journal of Portfolio Management*, 44(1):15–29, 2017. doi: 10.3905/jpm.2017.44.1.015.

- N. Jegadeesh and S. Titman. Returns to buying winners and selling losers: Implications for stock market efficiency. *The Journal of finance*, 48(1):65–91, 1993.
- A. Kirilenko, A. S. Kyle, M. Samadi, and T. Tuzun. The flash crash: High-frequency trading in an electronic market. *The Journal of Finance*, 72(3):967–998, 2017.
- R. A. Korajczyk and D. Murphy. High-frequency market making to large institutional trades. *The Review of Financial Studies*, 32(3):1034–1067, 2019.
- B. LeBaron. Some relations between volatility and serial correlations in stock market returns. *Journal of Business*, pages 199–219, 1992a.
- B. D. LeBaron. *Persistence of the Dow Jones index on rising volume*. University of Wisconsin Madison, WI, USA, 1992b.
- Y. Lempérière, C. Deremble, P. Seager, M. Potters, and J.-P. Bouchaud. Two centuries of trend following. *Journal of Investment Strategies*, 3(3):41–61, 2014. doi: 10.21314/JOIS.2014.043.
- A. Levine and L. H. Pedersen. Which trend is your friend? *Financial Analysts Journal*, 72(3): 51–66, 2016.
- J. C. Lorenzen, S. M. Kessler, M. Hornbach, A. tentes, K. Qian, and M. Liu. Understanding cta positioning and forecasting cta flows. *Morgan Stanley Research*, 2025.
- A. J. Menkveld. High frequency trading and the new market makers. *Journal of financial Markets*, 16(4):712–740, 2013.
- M. Mitchell and T. Pulvino. Arbitrage crashes and the speed of capital. *Journal of Financial Economics*, 104(3):469–490, 2012.
- T. J. Moskowitz, Y. H. Ooi, and L. H. Pedersen. Time series momentum. *Journal of financial economics*, 104(2):228–250, 2012.
- F. Patzelt and J.-P. Bouchaud. Universal scaling and nonlinearity of aggregate price impact in financial markets. *Physical Review E*, 97(1):012304, 2018.
- Quantica Capital. The footprint of trend-following: Can ctas really move the market? *Quantica Capital Quarterly Insights*, dec 2022. URL [https://quantica-capital.com/publications/pdf/2022Q4\\_QuanticaQuarterlyInsights.pdf](https://quantica-capital.com/publications/pdf/2022Q4_QuanticaQuarterlyInsights.pdf).
- Quantica Capital. When trend-following hits capacity: A case study on commodities. *Quantica Capital Quarterly Insights*, mar 2025. URL [https://quantica-capital.com/publications/pdf/2025Q1\\_QuanticaQuarterlyInsights.pdf](https://quantica-capital.com/publications/pdf/2025Q1_QuanticaQuarterlyInsights.pdf).
- C. Schmidhuber. Trends, reversion, and critical phenomena in financial markets. *Physica A: Statistical Mechanics and its Applications*, 566:125642, 2021.
- Société Générale Prime Services & Clearing. SG Prime Services Indices. URL <https://wholesale.banking.societegenerale.com/en/prime-services-indices/,urldate={2024-08-31}>.
- B. Tóth, Y. Lemperiere, C. Deremble, J. De Lataillade, J. Kockelkoren, and J.-P. Bouchaud. Anomalous price impact and the critical nature of liquidity in financial markets. *Physical Review X*, 1(2):021006, 2011.
- P. Van der Beck, J.-P. Bouchaud, and D. Villamaina. Ponzi funds. *arXiv preprint arXiv:2405.12768*, 2024.

- V. Van Kervel and A. J. Menkveld. High-frequency trading around large institutional orders. *The Journal of Finance*, 74(3):1091–1137, 2019.
- V. Volpati, M. Benzaquen, Z. Eisler, I. Mastromatteo, B. Tóth, and J.-P. Bouchaud. Zooming in on equity factor crowding. *arXiv preprint arXiv:2001.04185*, 2020.

## A Data

**Daily data.** All signal construction, portfolio simulation, and tick-size analyses use daily settlement prices and (daily reported) ticks for the following 101 futures contracts, spanning the four sectors introduced in Sec. 2 (commodities, equity indices, currencies, and government bonds/yields):

10USNOTE, 10YCAN, 2USNOTES, 5USNOTES, AEX, AUD, AUS10YR, AUS3YR, BOBL, BRENT0, BUND, BUSDBRL0, BUXL, CAC, CANOLA0, CCRUDE\_OIL0, CD, CHF, CIRON\_ORE0, COPPER0, CORN0, CPALM\_OIL0, CPTA0, CRAPESEEDM0, CRAPESEED00, CRUDE0, CSOYBEAN\_OIL0, CSOYMEAL0, DAX, DJMINI, EUR, EUROSTOXX, FCATTLE0, FRA10YR, FTSE, FTSEJSE40, FTSE\_CHINA\_A50, FTSE\_TAIWAN, GASOIL0, GBP, GILTS, GOLD0, HANGSENG, HEATOIL0, HRW0, HSHARES, IBEX, INSE\_NIFTY, ITA10YR, ITA3YR, JGB, JPY, KOR10YR, KOSPI, KRW, KTB3YR, LCATTLE0, LCOCOA0, LCOFFEE0, LEANHOGS0, LSUGAR0, MBOVESPA, MIB, MNIKKEI, MSCIEMINI, MSCIS, MXP, NATGAS0, NATGAS\_TTF0, NATGAS\_UK0, NCOCCOA0, NCOFFEE0, NCOTTON0, NFCOJ0, NIKKEI, NIKKEIS, NSDQMINI, NSUGAR0, NZD, PALADIUM0, PLATINUM0, PRAPSEED0, PWHEAT0, RBGASOL0, RUSSELLMINI, SCHATZ, SILVER0, SMI, SOYBEANM0, SOYBEANO0, SOYBEANS0, SPI200, SPMID, SPMINI, SPTSE60, TBOND, TOPIX, UTBOND, UTNOTE, WHEAT0, WTICRUDE0.

**Intraday bar data.** All order-book and order-flow analyses (Sec. 4.3 and Sec. 6) use proprietary 5-minute bar data from Capital Fund Management (CFM). Bar data are available for a smaller subset of contracts and over a shorter history than the daily series. We restrict the bar-data universe to contracts for which coverage begins no later than 2004, ensuring at least five years of pre-break data. This yields the following 53 contracts:

10USNOTE, 10YCAN, 2USNOTES, 5USNOTES, AUD, AUS3YR, BOBL, BRENT0, CD, CHF, COPPER0, CORN0, CRUDE0, DJMINI, EUR, FCATTLE0, FTSE, GASOIL0, GBP, GILTS, GOLD0, HANGSENG, HEATOIL0, HSHARES, JPY, KOSPI, KRW, KTB3YR, LCATTLE0, LCOCOA0, LCOFFEE0, LSUGAR0, MIB, MNIKKEI, MSCIS, MXP, NATGAS0, NCOCCOA0, NCOFFEE0, NCOTTON0, NIKKEI, NSDQMINI, NZD, RBGASOL0, RUSSELLMINI, SCHATZ, SILVER0, SPMINI, SPTSE60, TBOND, TOPIX, WHEAT0, WTICRUDE0.

Each 5-minute bar reports, per contract, the total traded volume, the buyer- and seller-initiated volumes (cumulative over the interval), and end-of-interval snapshots of the mid-price and of the resting volumes at the best bid and best ask.

## B Capacity Drag Calculation

In this appendix, it is roughly quantified that the execution-cost drag implied by the square-root impact law is rather insufficient to explain the observed PnL collapse.

Assuming, on any given day, that the CTA industry trades a total quantity  $Q$  over a time interval  $[0, T]$ , starting from a initial position  $q(0) = 0$  and finishing with an aggregate position  $Q = q(T) = \int_0^T \dot{q}(t)dt$ , where  $\dot{q}$  are the trades (here in continuous time), then under the square-root impact model as in Tóth et al. (2011), the total price change due to the CTAs should

be

$$p(T) = p(0) + \left( \frac{1}{V_d} \int_0^T \dot{q}(t) dt \right)^{1/2} \sigma_d Y + \text{noise}, \quad (9)$$

where  $V_d$  is the daily traded volume,  $\sigma_d$  is the daily volatility as a percentage of price (and thus in units of price:  $[\sigma_d] = [p] = \$$ ), and  $Y \approx 1$  is an empirical constant. The noise process is zero-mean.

The most basic execution schedule, following a constant trading rate,  $\dot{q} = \text{const}$ , implies  $\dot{q} = Q/T$ , such that  $q(t) = Q \frac{t}{T}$ . Under this model, the expected price impact reads

$$\mathcal{I}(t) = \mathbb{E}[p(t) - p(0)] = \left( \frac{Q}{V_d \frac{t}{T}} \right)^{1/2} \sigma_d Y. \quad (10)$$

The associated slippage or the impact-associated cost due to trading the entire position is

$$S(Q; T) = \mathbb{E} \left[ \int_0^T (p(t) - p(0)) \underbrace{\dot{q}(t)}_{= \frac{Q}{T}} dt \right] \quad (11)$$

$$= \int_0^T \left( \frac{Q}{V_d \frac{t}{T}} \right)^{1/2} \sigma_d Y \frac{Q}{T} dt = \frac{2}{3} \sigma_d Y \frac{Q^{3/2}}{V_d^{1/2}} \equiv S(Q), \quad (12)$$

implying a unit trading cost of

$$\bar{S} = \frac{S}{Q} = \frac{2}{3} \sigma_d Y \sqrt{\frac{Q}{V_d}} \quad (13)$$

Therefore, the slippage in terms of daily volatility, which is unit-less, is the following for a participation rate of  $1\% = \frac{Q}{V}$

$$\frac{\bar{S}}{\sigma_d} = \frac{2}{3} Y \sqrt{\frac{Q}{V_d}} = \frac{2}{3} 1 \sqrt{0.01} = \frac{2}{30}. \quad (14)$$

The annualised CTA trading cost, assuming 252 trading days, consequently is

$$\mathcal{C}_{\text{ann}} = \frac{2}{30} \mathcal{R}_d \cdot \text{turnover} \cdot 252 \quad (15)$$

with a turnover,  $\frac{\langle \Delta q \rangle}{\langle |q| \rangle}$ , that is the fraction of the total CTA daily risk that is typically traded daily. This figure is around 9% for the EWM-5-20 signal defined in Sec. ???.  $\mathcal{R}_d$  is the daily CTA risk. With an annualised CTA risk of  $\mathcal{R}_{\text{ann}} = \sqrt{252} \mathcal{R}_d$ , the reduction in Sharpe ratio expected from this simple calculation with a participation rate of 1% is

$$\Delta \text{Sharpe} = -\frac{\mathcal{C}_{\text{ann}}}{\sqrt{252} \mathcal{R}_d} = -\frac{2}{30} 9\% \sqrt{252} \approx -0.1. \quad (16)$$

The implied drag on Sharpe is therefore  $\sim 0.1$  at the observed industry participation rate of approximately 1%. This is non-trivial – it is roughly one-eighth of the pre-2009 trend Sharpe – but is too small, even when allowing for model uncertainty of a factor of three to four, to explain the observed collapse from  $\sim 0.7$  to  $\sim 0$ , even though the above should be treated rather as an order-of-magnitude calculation than a precise estimation.

## C Volume-clock Decomposition

The cumulative correlations of Sec. 4.3 aggregate over the full trading day and may therefore be diluted if the flow they aim to detect is localised intra-day. Industry lore suggests that CTAs execute the bulk of their daily volume in the opening hours of the underlying cash markets; during that window their trades would be strongly correlated with the prevailing order-flow state, while during the remaining hours the correlation would be significantly lower. The daily-aggregate correlation then reflects, at best, a weighted average of a concentrated within-window signal and a long stretch of noise, mechanically underestimating the intra-day effect.

To probe any such structure, a *volume-clock* is constructed. Because liquidity in futures is highly concentrated around the open of the underlying cash markets, a time-clock partition would assign vastly different volumes – and, therefore, vastly different signal-to-noise ratios – to intervals of equal duration. A volume-clock partition, on the contrary, assigns equal numbers of trades to each segment, making the corresponding correlations directly comparable across bins.

**Methodology.** For each product-day – defined according to the local trading day of the underlying cash market – we partition the 5-minute bars into five segments of equal traded volume, so that segment 0 contains the first 20% of daily volume, segment 1 the next 20%, and so on. Within each segment, the book and trade imbalances of Eq. (5) are recomputed using the segment’s own volume as the normalisation rather than the daily one. The cumulative correlations between the daily CTA trades  $\Delta\pi^{\text{CTA},\tau}$  and these segment-imbalances are then calculated as in Sec. 4.3, separately for each of the four asset classes and for four signal time scales  $\tau \in \{5, 10, 20, 50\}$ . Figs. 15 and 16 report the results.

**Findings.** Two features stand out.

*First, the asset-class heterogeneity persists.* For neither imbalance does a single consistent picture emerge across CMD, FXR, IDX, and YLD. The volume-clock decomposition does not resolve the cross-sectional inconsistency identified in Sec. 4.3; if anything, it reinforces it. This is, by itself, an important negative result: even the temporally most localised version of the H3 diagnostic fails to map the asset-class pattern of the order-flow regime change onto the asset-class pattern of PnL degradation.

*Second, volume bin 0 is an intra-day outlier systematically.* This is the most consistent feature across asset classes – though its direction varies – and is most conspicuous in the trade-imbalance decomposition (Fig. 15):

- For CMD, segment 0 reaches the highest cumulative correlation in the pre-2016 regime ( $\sim +0.4$  for EWM-5-20) and is the only segment that does not change sign afterwards.
- For FXR, segment 0 stands out from 2009 onwards, with the largest (negative) cumulative correlation across signal speeds; segment 0 already turns negative around 2009, while the other segments only join from 2016.
- For IDX, segment 0 is the most negative, reaching  $\sim -0.7$  for EWM-5-20, while other segments cluster at less negative or near-zero values.
- For YLD, segment 0 does not stand out particularly.

The book-imbalance decomposition (Fig. 16) shows qualitatively the same pattern: segment 0 is systematically the outlier – most positive for FXR and IDX fast signals, in line with leaders for YLD, and clustered with mid-segments for CMD.

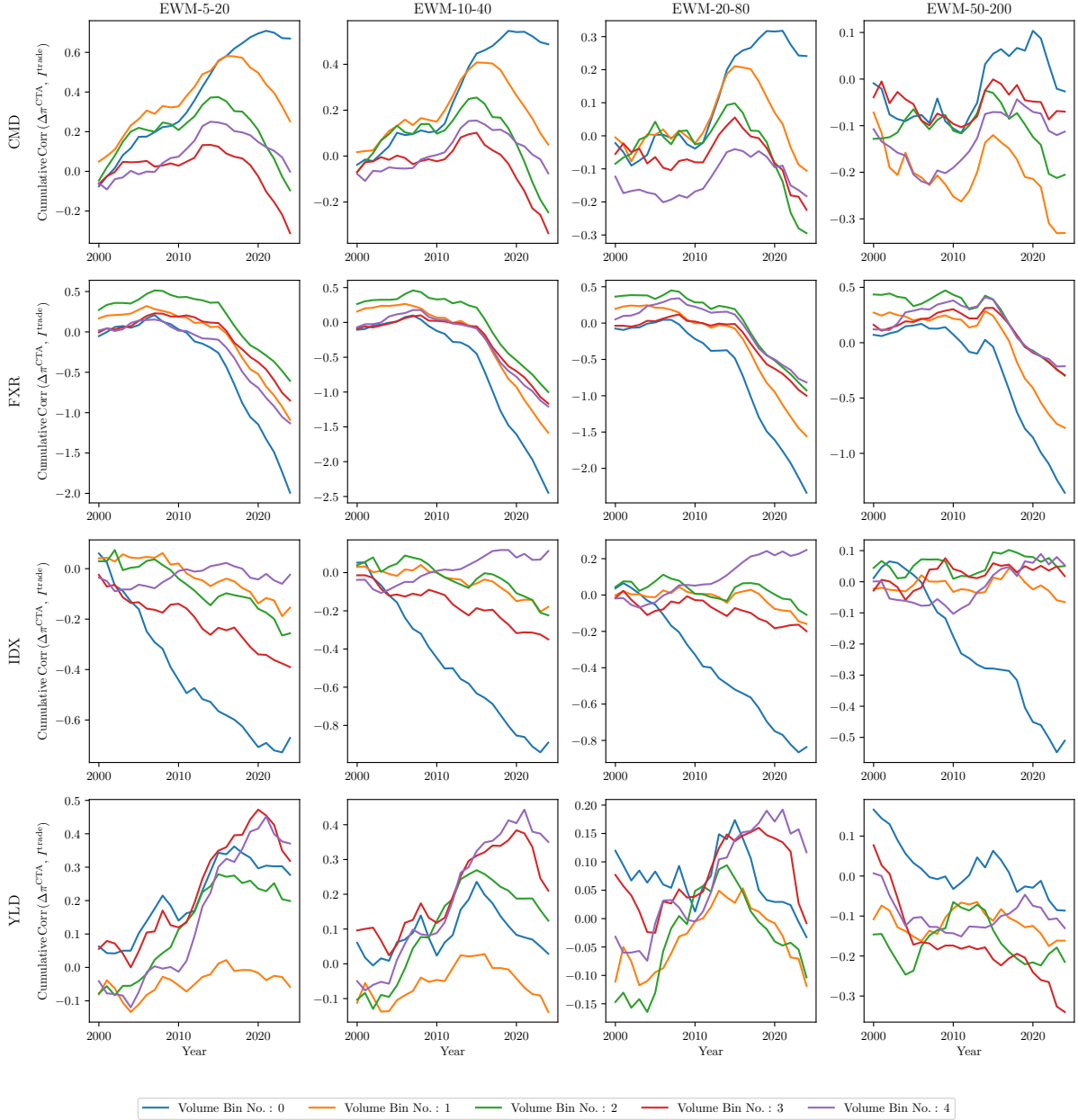


Figure 15: Cumulative correlations between daily CTA trades and the volume-weighted *trade* imbalance computed within 20%-of-volume intra-day segments, by asset class (rows: CMD, FXR, IDX, YLD) and signal time scale (columns: EWM- $\tau$ - $4\tau$  with  $\tau \in \{5, 10, 20, 50\}$ ). Volume bin 0 (blue) contains the first 20% of daily volume.

**Comparison with the daily aggregates.** The segment-wise correlations in Figs. 15 and 16 are broadly comparable in magnitude to the daily-average per-asset-class correlations of Fig. 9. The volume-clock decomposition therefore does not reveal an intra-day-localised effect that the daily aggregation had been underestimating. What it does reveal is intra-day structure – specifically, that the first 20% of daily volume behaves systematically differently from the remaining four segments – which is masked in the daily average. In that sense the segmentation refines the diagnostic without amplifying it.

**Interpretation.** Two readings are consistent with the extremity of segment 0.

(a) *CTA flow is intraday-concentrated.* If CTAs execute a disproportionate share of their

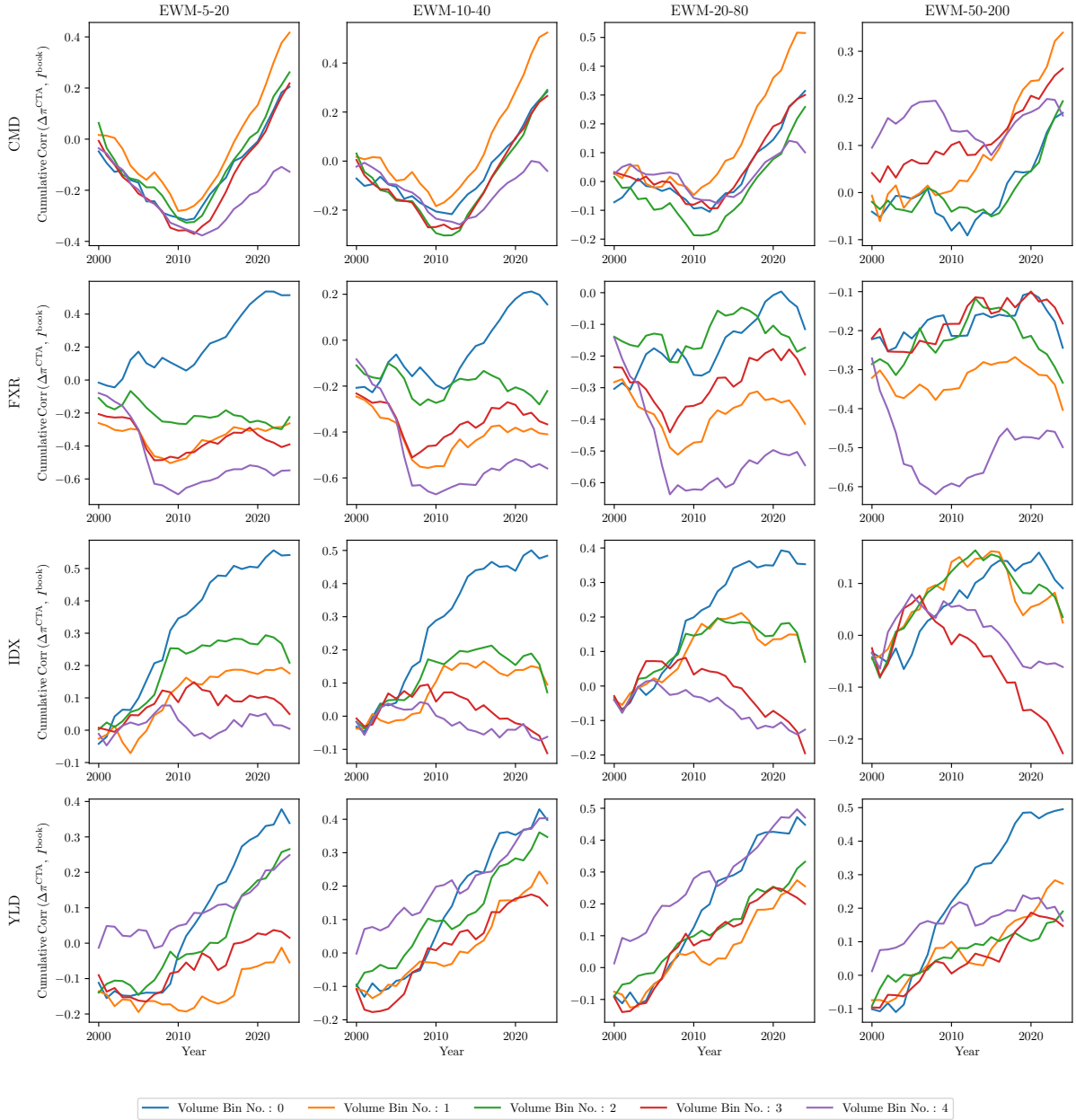


Figure 16: Same as Fig. 15 but for the volume-weighted *book* imbalance.

daily volume within segment 0 – as industry lore suggests – the correlation of their daily trades with the segment-0 imbalance is mechanically larger in magnitude than with segments where CTA activity is sparser. The sign of that correlation can in principle be sector-specific because the structure of liquidity provision at the open is itself asset-class-specific.

(b) *Segment 0 is structurally special.* The first 20% of daily volume generally subsumes the overnight carry-over period and the high-volume opening of the underlying cash market – periods of elevated volatility, liquidity fragmentation, and news incorporation. The order-flow statistics of segment 0 can therefore differ from those of segments 1–4 for reasons that have nothing to do with CTAs: any daily-aggregate flow would correlate differently with the segment-0 imbalance than with the others.

These readings are not mutually exclusive, and the data cannot cleanly attribute the bin-0 effect to one or the other. A decisive test of (a) would require knowledge of the actual intra-day distribution of CTA execution volume, which we do not have. What we can say is that the

volume-clock result is consistent with the folklore of morning-concentrated CTA execution and constitutes – to our knowledge – the first systematic empirical support for it in the academic literature on futures (a similar concentration has been previously established for institutional equity flow by Heston et al. (2010) and Bogousslavsky (2016)).

## D Within-contract Decompositions

For the tick size tiering that builds the groundwork in Sec. 5 is volatility-dependent, it is a natural concern whether the relationship between tick size and trend PnL goes yet deeper. Even within single contracts periods of high and low volatility – impacting the liquidity-tier ranking through the denominator – may correspond to different microstructural regimes, and may even have different PnL responses. This is was already alluded to in the final subsection of Sec. ?? but is analysed here further. Beyond the volatility-decomposition, a second decomposition of the PnL into large- and small-return days is investigated, which will also constraint any mechanism attempting to explain trend performance decay.

### D.1 Decomposition by Volatility Regime

For each contract  $i$ , a backward-looking (causal) rolling median  $\sigma_i^{\text{med}}(t)$  is computed on the last trading year (252 trading days). Based on this median, the trading days are partitioned into two similarly sized groups: a high-volatility ( $\sigma_i(t) > \sigma_i^{\text{med}}(t - 1)$ ) section and a low-volatility section, the complementary case. The cumulative trend PnL is then computed on each sub-sample separately. The results for different trend signals are depicted in Fig. 17.

Several observations strike:

1. Across all groups, low-volatility days contribute a disproportionate amount to the gains. In large tick contracts the vast majority of PnL comes from periods of low volatility across all signal horizons. For small ticks the same holds true pre-2009, and even after the PnL break is less bad in low-volatility regimes.

This observation is a strong cross-sectional confirmation of the *LeBaron effect* (LeBaron, 1992a,b), which states that many systematic trading rules, including trend, perform better in low-volatility regimes. For some cross-sections, especially large ticks, and also small ticks, this effect seems to even have strengthened post-break as the distance between the low and high volatility curves have widened.

2. While the all-days PnL and even more so the high-volatility PnL has collapsed are even gone negative for small ticks, the low-volatility PnL continues to accrue, even if at a lower rate. Therefore, the post-2008 PnL collapse on small tick contracts can be attributed to high-volatility days.
3. Small tick contracts behave qualitatively more like large tick products in periods of low-volatility. This observation may be interpreted as a confirmation of the effectiveness of the cross-sectional division based on  $\Psi/\sigma_i$  (instead of  $\sigma_i$  alone). Low-volatility periods correspond to a higher ratio, and on those days the LOBs of usually small tick products relatively resemble those of large tick products more closely in the microstructural sense and. The small tick trend PnL on those days also resembles the large tick one.

### D.2 Decomposition by Return Magnitude

The previous decomposition by volatility level hints at when the trend gains are collected. The next composition based on return magnitude shows from what kind of price changes trend

gains are collected from. A product  $i$  is classified as *large-return* when its current (volatility-normalised) absolute return is lower than the  $1\sigma$ -threshold calculated causally based on the last 252 trading days, i.e. when  $|r_i(t)| > 1\sigma_i^{\text{ann}}(t-1)$  and *small-return* in the complementary case.

Fig. 18 reports the result, which is genuinely striking. The small-return-day PnL contribution is utterly *invariant* to the trend break for all signals and for both tick size tiers. The small-return-PnL accrues at a nearly constant rate for the entire observation period 1995-2025, with no kink at the 2008/9 PnL break point, no acceleration during the 2008, 2014, or 2020 directional period, and no downturn after. In stark contrast stands the large-return-PnL that is responsible for basically all of the aberrations in the all-day PnL.

This allows for two important take-aways:

1. The trend break is a phenomenon of large-return days, not of the underlying signal.
2. The post-2008 regime shift has selectively eliminated trend followers' ability to profit

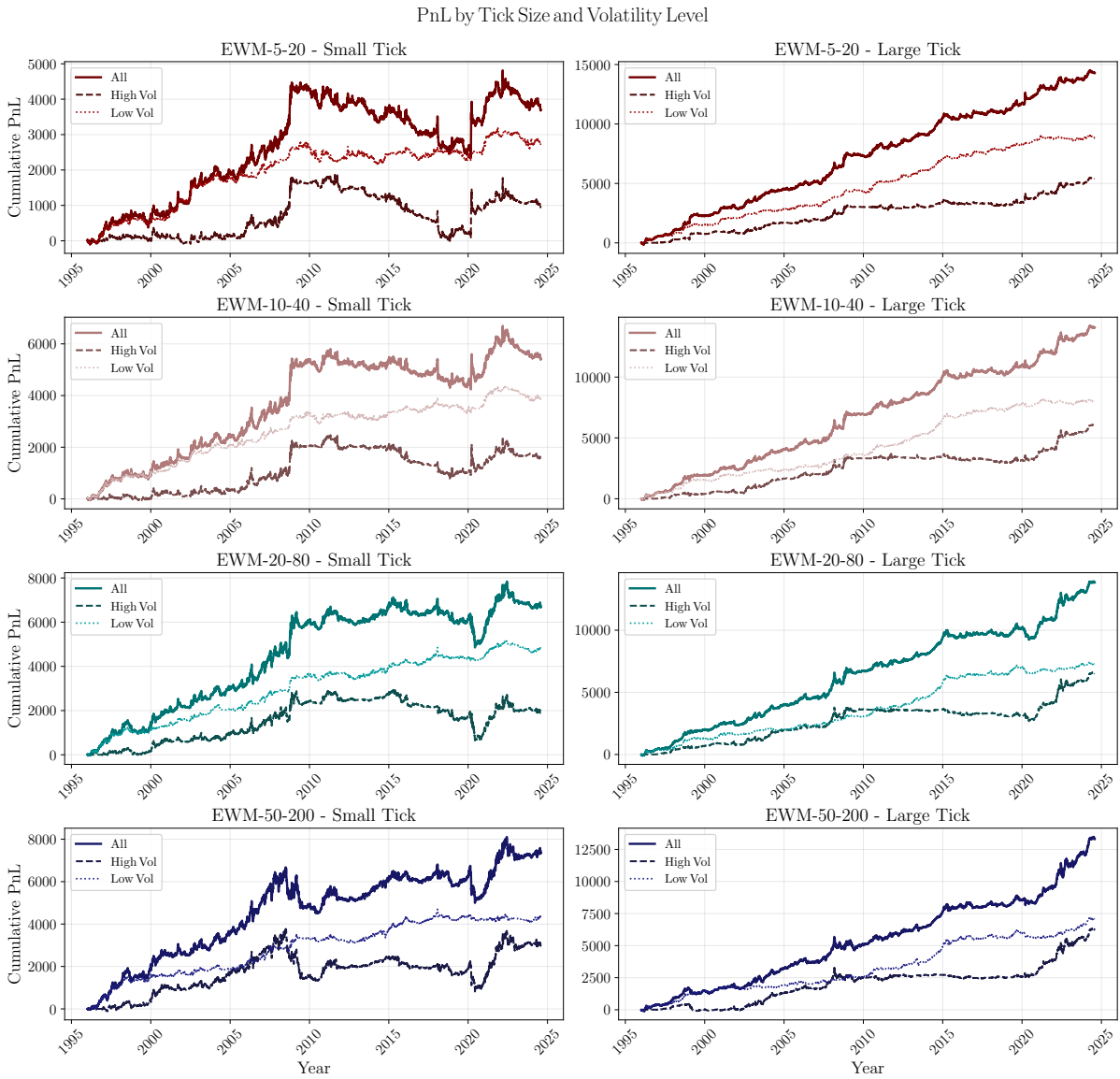


Figure 17: Cumulative trend PnL (non-liquidity-weighted portfolio, Eq. (2)) decomposed into contributions from high-volatility and low-volatility days. Rows: signal horizon EWM- $\tau$ - $4\tau$ . Left column: small-tick tier. Right column: large-tick tier. The volatility regime is defined per-contract per-year using the median realised volatility, computed causally.

from large price swings – exactly the moves that previously allowed for the strategy’s profitability.

This imposes a stronger empirical constraint on the explanatory mechanism than the all-day PnL would alone: whatever the mechanism, it must selectively impact trend followers on large-return days, and must leave the strategy’s performance under small returns unaffected.

Fig. 18 reports exactly that cross-sectional pattern.

Both decompositions therefore confirm the methodology deployed and consequences drawn: the volatility decomposition confirms  $\Psi_i/\sigma_i$  as the relevant microstructural variable, while the one by return magnitude highlights how trends stopped being predictive of large returns, thus significantly chipping away at the overall trend profitability.

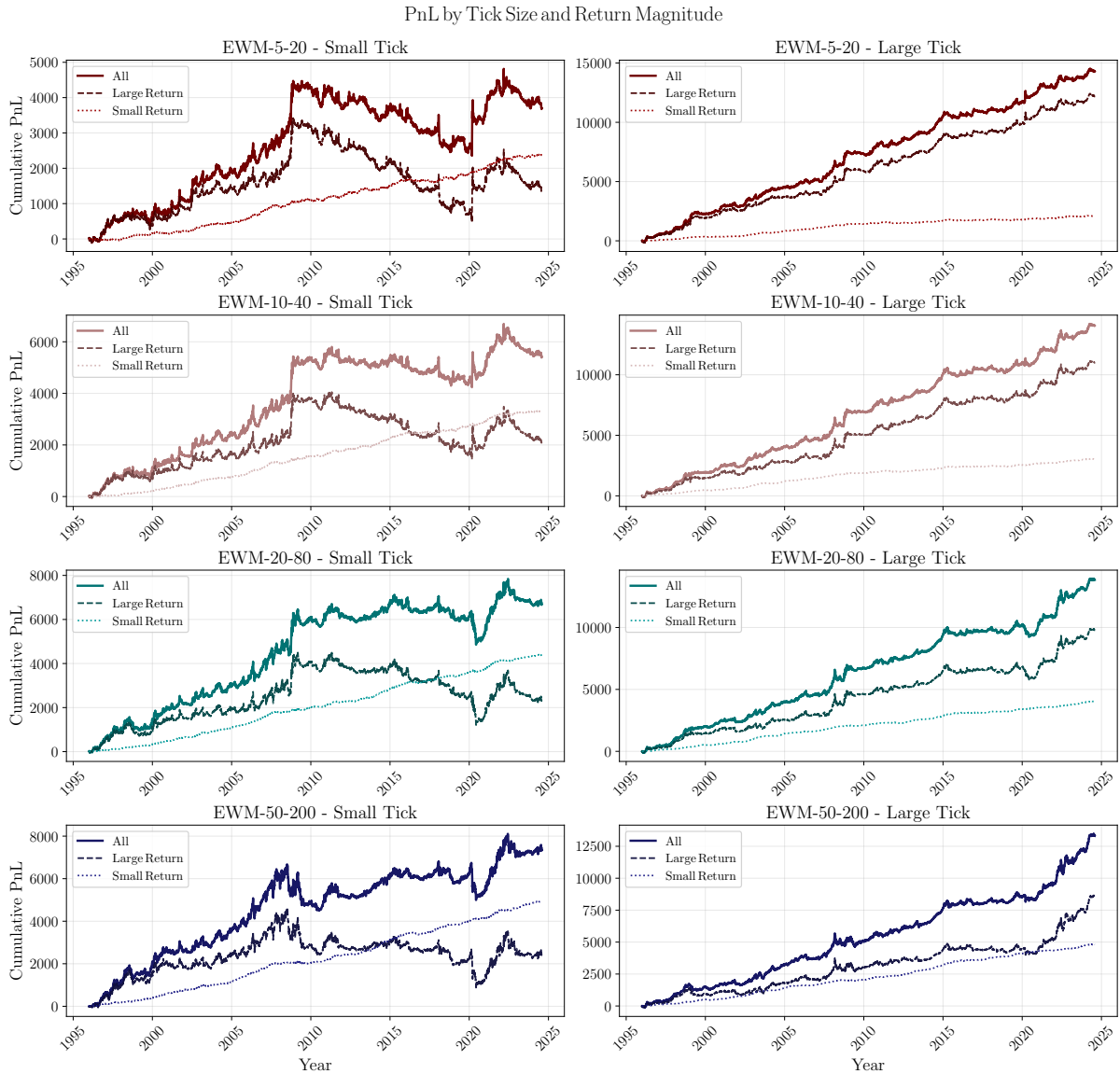


Figure 18: Cumulative trend PnL (non-liquidity-weighted portfolio, Eq. (2)) decomposed into contributions from high-volatility and low-volatility days. Rows: signal horizon EWM- $\tau$ - $4\tau$ . Left column: small-tick tier. Right column: large-tick tier. The volatility regime is defined per-contract per-year using the median realised volatility, computed causally.

## E Liquidity Tier Decomposition

Fig. 19 graphically confirms the negative correlation between liquidity and tick size, because of which a trend analysis based on liquidity instead of tick size was investigated.

From the figure three aspects may be inferred: First, liquidity and volatility-normalised ticksize are anti-correlated with a Pearson-correlation of  $-(35 \pm 8)\%$  in log-log-scale. This means that more liquid contracts tend to have smaller volatility-normalised tick sizes. Second, (volatility-normalised) tick size has decreased over the years. Third, overall liquidity has increased markedly during the considered time span. The last two observations are known facts.

Fig. 20 shows decisively that a partition into high and low liquidity products does not explain trend degradation as well as (volatility-normalised) tick size in Sec. 5, Fig. 10. One caveat is that all 101 contracts in our universe are relatively liquid by construction: less standard, lower-liquidity products that sit below the HFT market-makers' radar may well retain trend profitability. Such products, however, tend to fall in the large-tick category, so their inclusion would, if anything, reinforce rather than contradict the mechanism proposed in Sec.6.

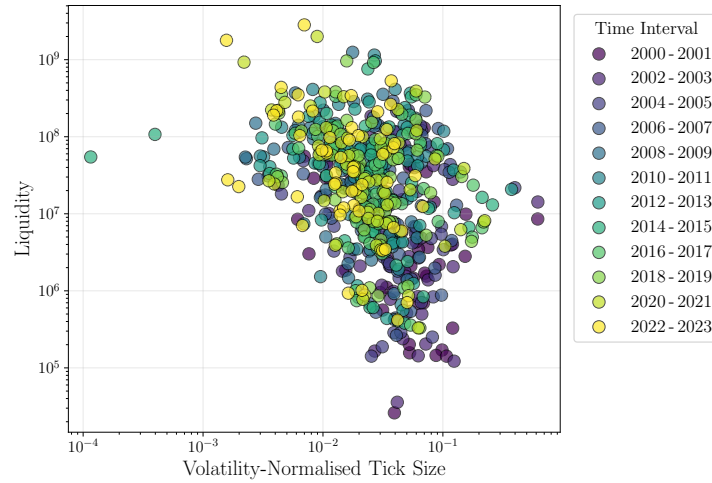


Figure 19: Liquidity vs. (volatility-normalised) tick size. The points are averaged in 2-year intervals. Axes are in log-scale; colours encode the progression in time.

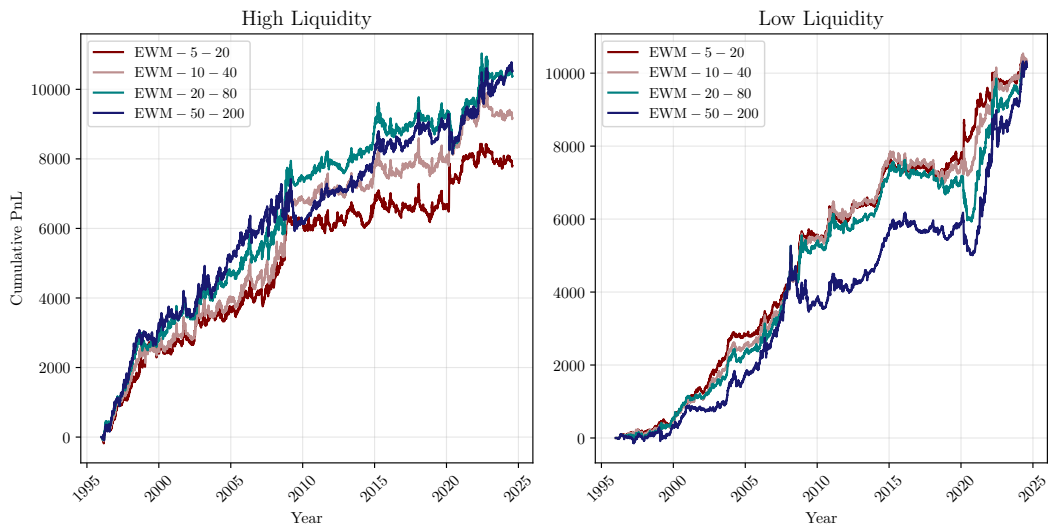


Figure 20: Cumulative PnL for different trend portfolios (not liquidity-weighted) and separated into two equal-sized liquidity tier. Tiering analogous to the procedure in Sec. 5 for the tick size.

## F Within-Asset-Class Tick-Tiered Performance

The tick size tiering procedure of Sec. 5 is repeated *within* each of the four asset classes, partitioning each sector's products into the 50% with the smallest and the 50% with the largest volatility-normalised tick size. A commodity classified as small-tick under this scheme therefore belongs to the lower half of the commodity cross-section, not necessarily to the lower half of the full universe.

Fig.21 collects the results, which corroborate the mechanism proposed in Sec.6 at higher resolution. Consistent with Fig.4, commodities and bonds outperform indices and currencies overall, which on our reading reflects their concentration in the large tick tier of the global universe. Bonds are an almost pure large tick sector: the within-sector tick split is therefore largely uninformative, and – as the mechanism predicts – neither sub-group shows appreciable degradation. The commodity cross-section is more heterogeneous, and the within-sector split is correspondingly more informative: the top row of Fig.21 shows that fast-trend PnL has degraded on the smaller tick half of the commodity universe while remaining intact on the larger tick half, mirroring the global dichotomy.

Indices and currencies, conversely, are concentrated in the global small tick tier and have, as documented in Sec.6 and Fig.4, lost fast-trend gains almost entirely. Yet even here the within-sector tiering carries signal in the expected direction: products classified as small-tick *within* IDX or FXR have degraded more than their large tick within-sector counterparts, even though both sub-groups sit on the small tick side of the global cross-section.

Together, these results suggest that the dependence of trend performance on volatility-normalised tick size is more gradual than the binary global split of Sec. 5 captures, and that tick size operates as a continuous microstructural variable rather than a dichotomous one. A finer tiering, or a fully continuous regression of post-break PnL on  $\Psi/\sigma$ , is a natural direction for future work.

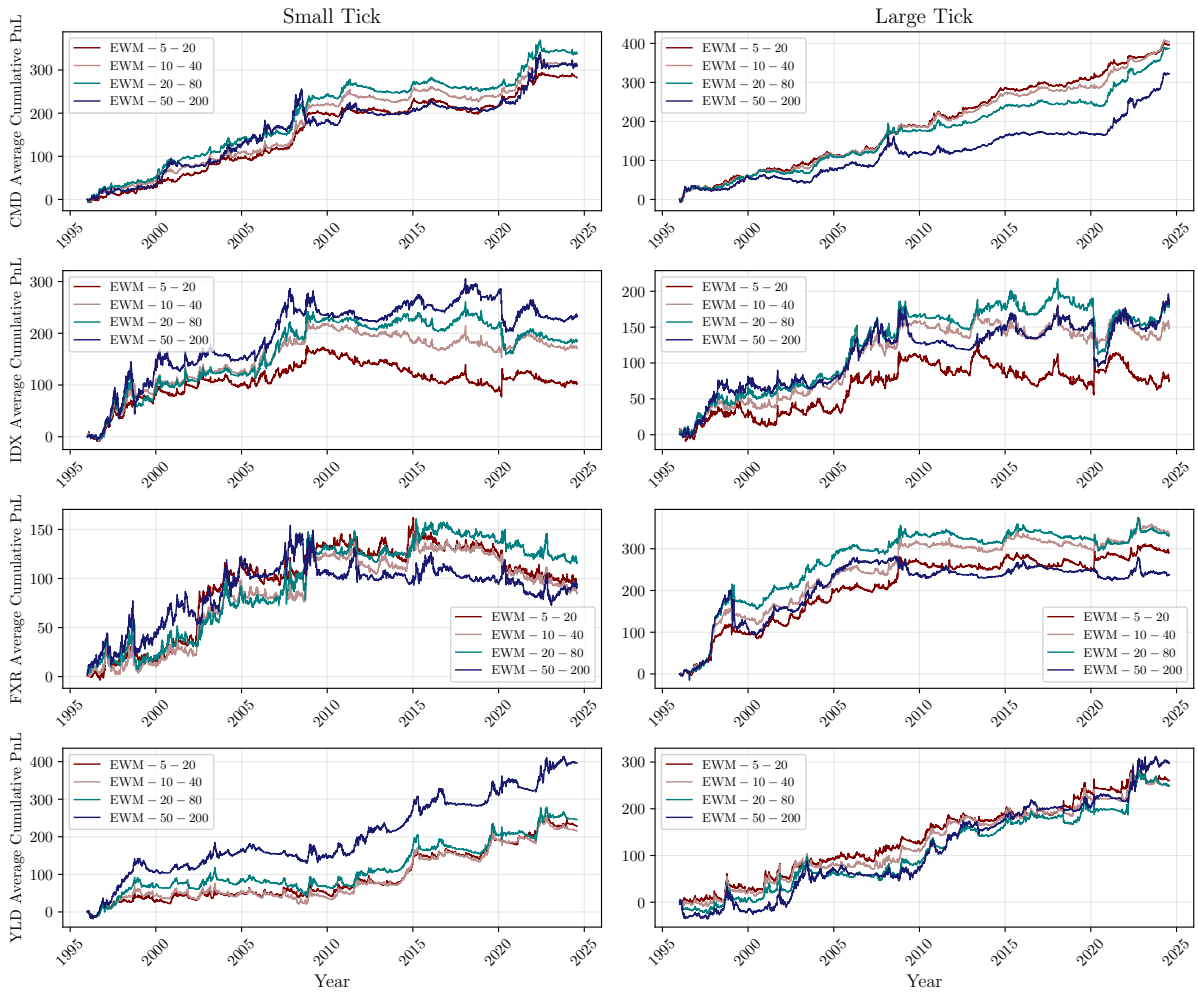


Figure 21: Same as Fig. 10 but with the tick-tiering performed per asset class.